Taylor & Francis
Taylor & Francis Group

RESEARCH ARTICLE

Check for updates

# Radiative transition probabilities between low-lying electronic states of N$_2$

Zhi Qin[a], Junming Zhao[a] and Linhua Liu[a,b]

[a]School of Energy Science and Engineering, Harbin Institute of Technology, Harbin, People's Republic of China; [b]School of Energy and Power Engineering, Shandong University, Qingdao, People's Republic of China

**ABSTRACT**

This work mainly investigates the transition dipole moments (TDMs) and radiative transition probabilities of dipole-allowed transitions between the b$^1\Pi_u$, a$''^1\Sigma_g^+$, 1$^3\Sigma_g^-$, 2$^3\Sigma_g^-$, 2$^3\Delta_g$, C$'^3\Pi_u$, B$'^3\Sigma_u^-$, W$^3\Delta_u$, 2$^3\Sigma_u^+$ and H$^3\Phi_u$ states of N$_2$. Many of these transition properties are previously unknown. For completeness, another 14 electronic states that correlate to four lowest dissociation limits are also calculated. The potential energy curves (PECs) are calculated at the valence internally contracted multireference configuration-interaction (icMRCI) level of theory, along with the Davidson correction, the core-valence (CV) correction and the scalar relativistic correction, as well as the basis-set extrapolation. These corrections, especially the CV correction, greatly improve the accuracy of the PECs, as shown by the excellent agreement of the fitted spectroscopic parameters with the available experimental data. In order to verify the accuracy of transition properties, we calculate the Einstein coefficients of the extensively studied B$^3\Pi_g$ − A$^3\Sigma_u^+$, C$^3\Pi_u$ − B$^3\Pi_g$, W$^3\Delta_u$ − B$^3\Pi_g$, B$'^3\Sigma_u^-$ − B$^3\Pi_g$, w$^1\Delta_u$ − a$^1\Pi_g$, a$^1\Pi_u$ − a$'^1\Sigma_u^-$, b$^1\Pi_u$ − X$^1\Sigma_g^+$ and b$^1\Sigma_u^+$ − X$^1\Sigma_g^+$ band transition systems and compute the radiative lifetimes of N$_2$B$^3\Pi_g$, C$^3\Pi_u$ and W$^3\Delta_u$ states, which are in good agreement with the experimental data. Similar accuracy can be assumed for the previously undetermined 1$^3\Sigma_g^-$ − C$'^3\Pi_u$, 2$^3\Sigma_g^-$ − C$'^3\Pi_u$, 2$^3\Sigma_g^-$ − B$'^3\Sigma_u^-$, 2$^3\Delta_g$ − W$^3\Delta_u$, 2$^3\Delta_g$ − H$^3\Phi_u$, 2$^3\Sigma_u^+$ − B$^3\Pi_g$ and b$^1\Pi_u$ − a$''^1\Sigma_g^+$ band transition systems. The large Einstein coefficients of these band systems can provide guidelines for observing such newly predicted band transitions in the appropriate spectroscopy experiments.
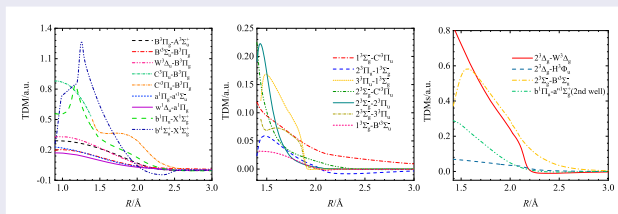
## I. Introduction

N$_2$ is one of the most widely studied homonuclear diatomic molecules due to its significance in the photophysical and photochemical processes taking place in stellar atmospheres [1–3], high-altitude nuclear explosion [4], gas discharge [5] and afterglows [6], etc. In addition, during the hypersonic flight into the Earth's atmosphere, radiation from high-temperature air in shock layers contributes to the heat flux suffered by the surface of the vehicles. Hence, radiation derived from high-temperature air must be predicted in order to efficiently design the thermal protection systems of vehicles [7–10]. It should be noted that radiative transition probabilities are important parameters to explain the atmospheric phenomena, to exploit the planetary spectra and to calculate the radiation. Hence, studies of the transition properties of N$_2$ are of crucial importance in these scientific research fields.

Numbers of experimental studies have been performed to measure the spectral transition properties of N$_2$. By organising the work of predecessors, Lofthus and Krupenie [11] gave a comprehensive review of the

experimental electronic spectra of $N_2$, which were later updated by Huber and Herzberg [12]. Subsequently, Neuschäfer et al. [13] observed an intense emission of the $B^3\Pi_g - A^3\Sigma_u^+$ transition from a nitrogen molecular beam which was passed through a dc discharge at the nozzle exit. Piper et al. [14] measured the relative variation in the transition dipole moment with internuclear distance for the $B^3\Pi_g - A^3\Sigma_u^+$ system by a branching-ratio technology. Fraser et al. [15] identified the $W^3\Delta_u$-$B^3\Pi_g$ band transition system by the Excede: Spectral auroral simulation experiment. And Ottinger and Vilesov [16] observed the $B^3\Pi_g - A^3\Sigma_u^+$ transition from metastable $N_2 A^3\Sigma_u^+$ component of a molecular beam and first determined the $N_2 A'^5\Sigma_g^+$ state experimentally by analysis of the perturbation. In addition, Roux et al. [17–24] measured the infrared emission spectrum of the $W^3\Delta_u - B^3\Pi_g$, $w^1\Delta_u - a^1\Pi_g$, $B^3\Pi_g - A^3\Sigma_u^+$ and $C^3\Pi_u - B^3\Pi_g$ transitions by high-resolution Fourier spectrometry. With the high-resolution laser-based one extreme-ultraviolet (EUV) + one UV two-photon ionisation spectroscopy and EUV photoabsorption spectroscopy, Lewis et al. [25] observed the C, $3s\sigma_g F_3$, and $3p\pi_u G_3{}^3\Pi_u$ Rydberg states and studied spin-forbidden $^3\Pi_u - X^1\Sigma_g^+$ transitions. Summarising the experimental results, we found that most experimental studies mainly investigated the $B^3\Pi_g - A^3\Sigma_u^+$, $C^3\Pi_u - B^3\Pi_g$ and $W^3\Delta_u - B^3\Pi_g$ band transition systems. Transition properties achieved by experiments are limited by the present technologies. Therefore, theoretical calculations need to be carried out in order to predict the theoretically possible transitions and to provide guidance for observing the unknown transitions by appropriate spectroscopy experiments.

To calculate the transition properties of diatomic molecules, many theoretical approaches have been developed. The earlier valence configuration interaction (VCI) treatment of Michels [26] and configuration interaction (CI) study of Ermler et al. [27] presented a more complete treatment of the $N_2$ electronic states, including the potential energy curves of low-lying valence states, the dominant molecular-orbital configurations and a listing of known and predicted spectroscopic data. Werner et al. [28] employed the multi-configuration self-consistent field (MCSCF) and self-consistent electron pairs (SCEP) methods to calculate the radiative transition probabilities of the $B^3\Pi_g - A^3\Sigma_u^+$, $C^3\Pi_u - B^3\Pi_g$, $W^3\Delta_u - B^3\Pi_g$ and $B'^3\Sigma_u^- - B^3\Pi_g$ band transition systems. The potential energy curves and transition moments of $^1\Sigma_g^+$ and $^1\Sigma_u^+$ were investigated with CI method by Ermler et al. [29]. Yet the CI method at that time was limited by the number of reference spaces, so a new internally contracted direct multiconfiguration-reference configuration interaction (MRCI) method was presented by Werner and Knowles [30,31], allowing the use of much larger reference spaces, thus promoting the efficiency and accuracy of the potential energy functions and molecular properties. With the MRCI method, Ndome et al. [32] calculated the diagonal spin–orbit functions for the lowest three non-Rydberg states of $^3\Pi_u$ symmetry in molecular nitrogen, which were consistent with the experimental data of Ref. [25]. Hochlaf et al. [33,34] computed the potential energy curves and spin–orbit coupling integrals of $N_2$ electronic states located in the 0–120000 $cm^{-1}$ energy domain and investigated the valence-Rydberg quintet states, the transition moments and the spin–orbit couplings to the close lying triplet electronic states. Shi et al. [35] studied the potential energy curves and the spectroscopic parameters of the $A^3\Sigma_u^+$, $B^3\Pi_g$, $W^3\Delta_u$ and $B'^3\Sigma_u^-$ states for the $^{14}N_2$, $^{14}N^{15}N$, $^{15}N_2$ isotopologues including the Davidson correction, the core-valence correction and the scalar relativistic correction. Moreover, Little and Tennyson [36] gave a detailed calculation of the potential energy curves for singlet and triplet Rydberg states of $N_2$ using three ab initio procedures.

However, most of the theoretical studies focused on the potential energy curves and the spectroscopic parameters. Only $B^3\Pi_g - A^3\Sigma_u^+$, $C^3\Pi_u - B^3\Pi_g$, $W^3\Delta_u - B^3\Pi_g$, $B'^3\Sigma_u^- - B^3\Pi_g$, $w^1\Delta_u - a^1\Pi_g$, $a^1\Pi_g - a'^1\Sigma_u^-$, $b^1\Pi_u - X^1\Sigma_g^+$ and $b^1\Sigma_u^+ - X^1\Sigma_g^+$ band transition systems have been investigated. In this paper, the state-of-the-art *ab-initio* methodology is used to mainly investigate the radiative transition properties of dipole-allowed transitions between the $b^1\Pi_u$, $a''^1\Sigma_g^+$, $1^3\Sigma_g^-$, $2^3\Sigma_g^-$, $2^3\Delta_g$, $C'^3\Pi_u$, $B'^3\Sigma_u^-$, $W^3\Delta_u$, $2^3\Sigma_u^+$ and $H^3\Phi_u$ states of $N_2$. The computational approaches are introduced in the next section. The potential energy curves (PECs) and spectroscopic parameters of these electronic states are calculated and given in section III A. In section III B, transition dipole moments (TDMs) are calculated and used to determine the radiative transition probabilities of dipole-allowed transitions between the $b^1\Pi_u$, $a''^1\Sigma_g^+$, $1^3\Sigma_g^-$, $2^3\Sigma_g^-$, $2^3\Delta_g$, $C'^3\Pi_u$, $B'^3\Sigma_u^-$, $W^3\Delta_u$, $2^3\Sigma_u^+$ and $H^3\Phi_u$ states of $N_2$. In section IV, conclusions are drawn.

## II. Computational approaches

All the *ab initio* electronic calculations of $N_2$ were carried out with the MOLPRO 2015 programme suite [37,38]. Potential energy curves were calculated using the complete active space self-consistent field (CASSCF) [39] method followed by the valence internally contracted MRCI (icMRCI) [30,31] approach with the Davidson correction [40]. All configuration state functions (CSFs)

obtained by CASSCF are used as a reference for the icM-RCI calculations. In CASSCF, the state-averaged technique is employed for the electronic states which have the same spin and symmetry. Both the aug-cc-pV5Z (AV5Z) and aug-cc-pV6Z (AV6Z) basis sets of Dunning [41–43] are used to describe the nitrogen atom for extrapolating the potential energies to the complete basis set (CBS) limit (described below).

The $N_2$ molecule belongs to $D_{\infty h}$ symmetry. However, we must replace the $D_{\infty h}$ symmetry with the $D_{2h}$ point group due to the limitation of the programme. The corresponding symmetry operations for the $D_{\infty h} \rightarrow D_{2h}$ can be found in Ref. [44]. In the calculations of the CASSCF and subsequent icMRCI, core-valence (CV) correlation energy correction and scalar relativistic energy correction, the valence molecular orbitals (MOs) and two more $\sigma_g$ and two more $\pi_u$ MOs were included into the active space, which had been proved to be more effective in treating the Rydberg character of the electronic states, especially for higher-lying electronic states [32–34,45].

In the icMRCI calculations, basis-set extrapolation was used to obtain more reliable and accurate potential energy curves. The potential energy for each internuclear distance comprises two parts: the reference energy and the correlation energy. Since the reference energy converges faster than the correlation energy, the reference and correlation energies should be extrapolated separately. We use the basis-set extrapolation formula [46,47], just as follows

$$E_X^{ref} = E_\infty^{ref} + A^{ref} X^{-\alpha}, \quad (1)$$

$$E_X^{cor} = E_\infty^{cor} + A^{cor} X^{-\beta}. \quad (2)$$

where $E_X^{\text{ref}}$ and $E_X^{\text{cor}}$ are the reference and correlation energies, respectively, which are calculated with the aug-cc-pVXZ basis set. $E_\infty^{\text{ref}}$ and $E_\infty^{\text{cor}}$ denote the reference and correlation energies, respectively, which are obtained by the extrapolation of the basis set to the CBS limit $\infty$. In this work, the aug-cc-pV5Z (AV5Z) and aug-cc-pV6Z (AV6Z) basis sets were adopted to extrapolate the potential energies (denoted as icMRCI + Q/56). $A^{ref}$ and $A^{cor}$ are constants for a given molecule. Extrapolated parameters $\alpha$ and $\beta$ are obtained from Truhlar [46] as 3.4 and 2.4 for the reference and correlation energies, respectively.

CV correlation energy correction was obtained by the icMRCI approach using the aug-cc-pCV5Z basis set [41]. The difference between the energy calculated by considering all the electrons in the two N atoms and that obtained by frozen-core calculation for the four electrons in the 1 s inner orbital of the two N atoms produces the CV correlation energy correction result. Scalar relativistic energy correction was calculated via the third-order Douglas–Kroll–Hess (DKH3) Hamiltonian approximation [48–50] at the icMRCI level of theory. More specifically, the aug-cc-pV5Z-DK basis set with the DKH3 approximation and the aug-cc-pV5Z basis set without the DKH3 approximation were both used to compute the potential energy. The difference between these two energies is the scalar relativistic energy correction result, denoted as DK.

Electronic transition dipole moments (TDMs) were calculated at the icMRCI/AV6Z level of theory. Utilising the PECs, the vibrational level energies can be obtained by solving the nuclear radial Schrödinger equation, and the rotational constant $B_v$ can be calculated by [51]

$$B_v = \left(\frac{\hbar}{2\mu}\right)\left\langle v,J \left| \frac{1}{r^2} \right| v,J \right\rangle \quad (3)$$

where $\hbar$ïÿĂ is the reduced Planck's constant, $\mu$ is the reduced mass of the molecule, $v$ and $J$ are the vibrational and rotational quantum number, respectively, and $r$ is the internuclear distance. By analysing the potential energy curve and fitting the vibrational level energies and the rotational constant as polynomials of $v + 1/2$, we obtained the spectroscopic parameters of electronic states, including adiabatic excitation energy $T_e$, dissociation energy $D_e$, equilibrium internuclear distance $r_e$, harmonic frequency $\omega_e$, first- and second-order anharmonic constants $\omega_e x_e$ and $\omega_e y_e$, balanced rotation constant $B_e$ and rovibrational coupling constant $\alpha_e$. With the calculated PECs and TDMs, radiative transition probabilities, i.e. Einstein coefficients of spontaneous emission (hereinafter referred to as Einstein coefficients), were determined by the LEVEL programme [51]. Einstein coefficients were then used to calculate the radiative lifetimes of different vibrational levels of some electronic states.

Note that a single barrier emerges in some electronic states, leading to different treatments of $D_e$ for different electronic states. If the barrier is higher than the dissociation limit, we determine the $D_e$ by the difference between the potential energy at the equilibrium internuclear distance and that at the top of the barrier. If not, the $D_e$ is evaluated by the difference between the potential energy at the equilibrium internuclear distance and that at the dissociation asymptote. The energy separations between each higher dissociation limit and the lowest one are calculated at the icMRCI + Q/56 + CV + DK theory level and given in Table 1.

As shown in Table 1, the obtained energy separations are in good agreement with the experimental data from Refs. [11] and [52].

**Table 1.** 7 Singlet and 17 triplet electronic states of $N_2$ and their dissociation limits.

| Dissociation limit | Electronic states | Relative energy (cm$^{-1}$) | |
|---|---|---|---|
| | | This work[a] | Exp.[11,52] |
| $N(^4S_u) + N(^4S_u)$ | $X^1\Sigma_g^+$, $A^3\Sigma_u^+$ | 0.00 | 0.00 |
| $N(^4S_u) + N(^2D_u)$ | $W^3\Delta_u$, $B^3\Pi_g$, $C^3\Pi_u$, $C'^3\Pi_u$, $E^3\Sigma_g^+$, $G^3\Delta_g$, $2^3\Sigma_u^+$ | 19258.55 | 19224.46 |
| $N(^4S_u) + N(^2P_u)$ | $B'^3\Sigma_u^-$, $1^3\Sigma_g^-$, $2^3\Pi_u$, $2^3\Pi_g$ | 28890.42 | 28839.31 |
| $N(^2D_u) + N(^2D_u)$ | $a^1\Pi_g$, $a'^1\Sigma_u^-$, $w^1\Delta_u$, $b^1\Pi_u$, $a''^1\Sigma_g^+$, $1^1\Gamma_g$, $H^3\Phi_u$, $2^3\Sigma_g^-$, $3^3\Pi_u$, $3^3\Pi_g$, $2^3\Delta_g$ | 38477.87 | 38448.93 |

[a]determined at the icMRCI + Q/56 + CV + DK level of theory.

## III. Results and discussion

### A. Potential energy curves and spectroscopic parameters

Potential energy curves of 7 singlet and 17 triplet electronic states calculated at the icMRCI + Q/56 + CV + DK level of theory are shown in Figure 1. For the electronic states that are vastly studied, we will not elaborate on them and just provide the calculated potential energies in the Supplementary Material. Some electronic states that are important for calculating the radiative transition parameters are elaborated below.

### 1. The $^3\Pi_u$ states

Predissociation of the $^3\Pi_u$ states for $N_2$ attracts the interests of many researchers due to its significance in the photochemistry of nitrogen-rich planetary atmospheres. Since Carroll and Mulliken [53] presented an insightful work of the structure and predissociation for the $^3\Pi_u$ states of $N_2$, a large number of experimental and theoretical studies [21,24,25,27,32,33,36,54–56] had been carried out on the $^3\Pi_u$ states and their strong mutual interactions. Nevertheless, the shapes of the potential energy curves for the $^3\Pi_u$ states remain controversial. The recent work from Little and Tennyson [36] presented a comparison of the $^3\Pi_u$ states with those of Hochlaf et al. [33]

and Guberman [56]. Obvious differences of the potential energy curves for the $^3\Pi_u$ states can be observed among these three calculations, especially for smaller internuclear distances as shown in Figure 2.
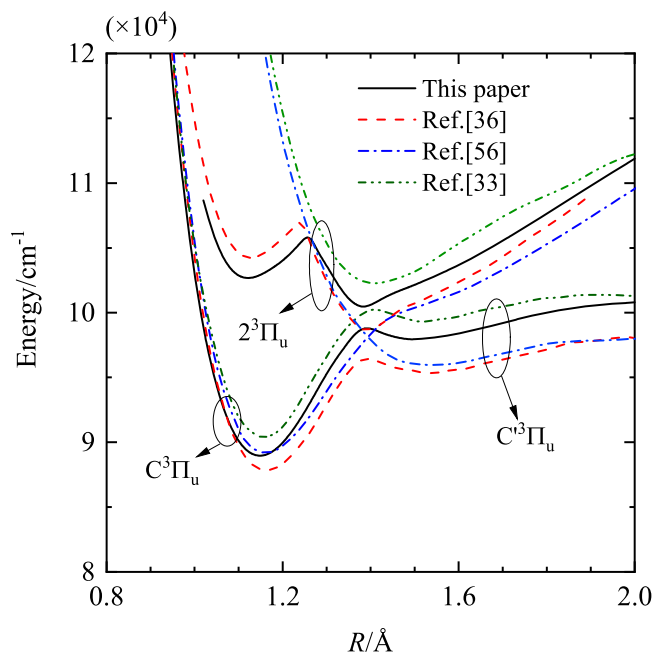
**Figure 2.** $N_2$ $C^3\Pi_u$, $C'^3\Pi_u$ and $2^3\Pi_u$ states compared to those of Little and Tennyson [36], Guberman [56] and Hochlaf et al. [33].
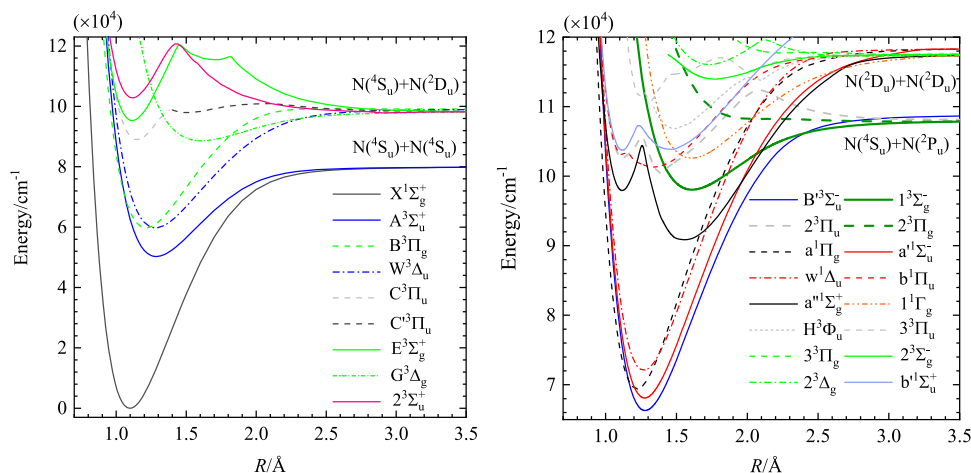
**Figure 1.** Potential energy curves of $N_2$ electronic states calculated at the icMRCI + Q/56 + CV + DK level of theory. The potential energy curves are given in energy relative to the minimum of the ground state.

For the $C^3\Pi_u$ state, the calculated potential energy curve is similar to previous theoretical ones. Its potential energy curve becomes inverted at an internuclear distance near 2.1Å, corresponding to a change in the leading electronic configuration from $(1\sigma_g)^2(1\sigma_u)^2(2\sigma_g)^2(2\sigma_u)$ $(3\sigma_g)^2(1\pi_u)^4(1\pi_g)$ to $(1\sigma_g)^2(1\sigma_u)^2(2\sigma_g)^2(2\sigma_u)^2(3\sigma_g)$ $(1\pi_u)^3(1\pi_g)^2$, thus forming a new state $C'^3\Pi_u$. Such feature had been studied in detail by Ndome et al. [32]. The calculated equilibrium distances of the $C^3\Pi_u$ and $C'^3\Pi_u$ states are 1.1480Å and 1.5111Å, respectively, which are in excellent agreement with the experimental values of 1.149Å and 1.514Å [12], respectively. The dissociation energy of the $C^3\Pi_u$ state obtained here is 9957.73 cm$^{-1}$, which is about 20 cm$^{-1}$ higher than the experimental value of 9978.51 cm$^{-1}$. The vibrational level energies and internal rotation constants of the $C^3\Pi_u$ state are given and compared with the experimental values [24] in the Supplementary Material, and good agreement is observed except for $\upsilon = 3$ and $\upsilon = 4$ for the $C^3\Pi_u$ state since there is a strong interaction between the $C^3\Pi_u$ and $C'^3\Pi_u$ states at internuclear distance near 1.3Å (corresponding to $\upsilon = 3$ and $\upsilon = 4$). For $2^3\Pi_u$ state, our icMRCI + Q/56 + CV + DK calculations of the potential energy curve is closer to those recently calculated using the UK molecular $R$-matrix method [36] for the internuclear distances lower than about 1.25Å. For the internuclear distances larger than 1.25Å, our calculated potential energy curve is similar to previous theoretical ones.

## 2. The $1^1\Gamma_g$ state

The electronic state of $1^1\Gamma_g$ was first mentioned theoretically by Ermler et al. [27]. Almost simultaneously, Michels [26] presented a full potential energy curve of the $1^1\Gamma_g$ state that is strongly bound with a deep potential well of 17582.88 cm$^{-1}$, updated to $\sim 13750$ cm$^{-1}$ by Hochlaf et al. [33] with the MRCI/aug-cc-pVQZ calculations. A potential well of 14758.27 cm$^{-1}$ is obtained in this work at the icMRCI + Q/56 + CV + DK level of theory. Our calculated excitation energy of the $1^1\Gamma_g$ state is 102590.25 cm$^{-1}$, which is about 400 cm$^{-1}$ lower than the calculated value of 102993 cm$^{-1}$ from Hochlaf et al. [33]. The calculated equilibrium distance is 1.6073Å, which is very close to the calculated one of Hochlaf et al. [33]. The first ten vibrational levels and inertial rotation constants are used to fit the spectroscopic constants: $\omega_e = 801.45$ cm$^{-1}$, $\omega_e x_e = 9.52$ cm$^{-1}$, $\omega_e y_e = 0.18$ cm$^{-1}$, $B_e = 0.92971$ cm$^{-1}$ and $\alpha_e = 0.931$ cm$^{-1}$ (Table 2). The $1^1\Gamma_g$ state is the double orbital excitation from the ground state and its wavefunction is dominated by the $(1\sigma_g)^2(1\sigma_u)^2(2\sigma_g)^2(2\sigma_u)^2(3\sigma_g)^2(1\pi_u)^2$ $(1\pi_g)^2$ electronic configuration, i.e. two electrons excite from the $(1\pi_u)$ MO into the vacant $(1\pi_g)$ MO.

## 3. The $^3\Sigma_g^-$ states

A $^3\Sigma_g^-$ state $(1^3\Sigma_g^-)$ that converges adiabatically to the $N(^4S_u) + N(^2P_u)$ dissociation limit was predicted by Michels [26] in 1981, confirmed about 30 years later by Hochlaf et al. [33] through the large calculations at the MRCI/aug-cc-pVQZ level of theory. This electronic state is formed after excitation of two electrons from the $(1\pi_u)$ MO into the $(1\pi_g)$ MO. Michels also predicted another $^3\Sigma_g^-$ state $(2^3\Sigma_g^-)$ with a double-well potential. The existence of this electronic state is confirmed by Hochlaf et al., but with a unique shallow potential well, which is also confirmed in our calculations at the icMRCI + Q/56 + CV + DK level of theory. And the $2^3\Sigma_g^-$ state is dominated by the $(1\pi_u)^{-2}(1\pi_g)^2$ and $(3\sigma_g)^{-2}(1\pi_g)^2$ electronic configurations. These two states were studied in detail by Hochlaf et al. [33] due to its important role in $N_2$ vacuum ultra violet (VUV) photodissociation. In our work, these two states are found to be very important for their radiative transitions to the $^3\Pi_u$ states. The radiative transition probabilities between the $^3\Sigma_g^-$ states and $^3\Pi_u$ states are given in section B.

## 4. The $^3\Sigma_u^+$ states

Among the states of the $^3\Sigma_u^+$ symmetry, the $A^3\Sigma_u^+$ state is mostly studied theoretically and experimentally [14,19,28,35,70] and will not be elaborated here. Michels [26] and Hochlaf et al. [33] predicted a $^3\Sigma_u^+$ state $(2^3\Sigma_u^+)$ that is nearly repulsive. However, an apparent potential well located at about 102792 cm$^{-1}$ for internuclear distances smaller than about 1.4 Å is found in this work. The depth of the potential well is 18000.63 cm$^{-1}$. The equilibrium distance of the $2^3\Sigma_u^+$ state is 1.1168 Å. The potential well is formed at internuclear distances where the corresponding potential energies have not been studied before. The existence of such a potential well maybe contributes to its radiative transition to the adjacent electronic states, e.g. the $2^3\Sigma_u^+ - E^3\Sigma_g^+$ transition is expected to be most likely to occur. In addition, the $3^3\Sigma_u^+$ state that correlates to the $N(^2D_u) + N(^2D_u)$ dissociation limit is predicted to exist lying higher than the $2^3\Sigma_u^+$ state, with a similar shape of the potential energy curve to that of the $2^3\Sigma_u^+$ state. The potential energy curve of the $3^3\Sigma_u^+$ state is not given here due to its uncertainty.

## 5. The $b^1\Pi_u$ and $b'^1\Sigma_u^+$ states

The calculated potential energy curves of the $b^1\Pi_u$ and $b'^1\Sigma_u^+$ electronic states are given in Figures 3 and 4, respectively, and compared with those of Little and Tennyson [36] and those of Spelsberg and Meyer [45]. For the $b^1\Pi_u$ state, our calculations predict a potential energy curve lower than previous theoretical data [36,45] for internuclear distances smaller than 1.13Å. Beyond this

**Table 2.** Spectroscopic parameters of the electronic states of $N_2$ calculated at the icMRCI + Q/56 + CV + DK level of theory and their comparison with available experimental and theoretical data.

| Electronic state | | $D_e$/cm$^{-1}$ | $T_e$/cm$^{-1}$ | $R_e$/Å | $\omega_e$/cm$^{-1}$ | $\omega_e x_e$/cm$^{-1}$ | $10^2\omega_e y_e$/cm$^{-1}$ | $B_e$/cm$^{-1}$ | $10^2\alpha_e$/cm$^{-1}$ |
|---|---|---|---|---|---|---|---|---|---|
| $X^1\Sigma_g^+$ | This paper | 79889.28 | 0.00 | 1.0975 | 2359.56 | 14.1093 | −1.369 | 1.99896 | 1.718 |
| | Exp. [11] | 79889.77 | 0.00 | 1.0977 | 2358.57 | 14.324 | −2.258 | 1.99820 | 1.728 |
| | Exp. [12] | | 0.00 | 1.0977 | 2358.57 | 14.324 | −2.26 | 1.99824 | 1.732 |
| | Cal. [57] | 70492.83[a] | 0.00[a] | 1.1201[a] | 2323[a] | | | | |
| | Cal. [58] | 79462[b] | 0.00[b] | 1.0994[b] | 2343[b] | | | | |
| | Cal. [59] | 80622.03[c] | 0.00[c] | 1.0984[c] | 2354.2[c] | | | | |
| $A^3\Sigma_u^+$ | This paper | 29621.03 | 50268.43 | 1.2862 | 1461.84 | 13.5119 | −3.929 | 1.45522 | 1.804 |
| | Exp. [11,60] | 29685.81 | 49754.78 | 1.2866 | 1460.64 | 13.8723 | −1.030 | 1.4546 | 1.799 |
| | Exp. [12] | | 50203.63 | 1.4546 | 1460.64 | 13.872 | | 1.4546 | 1.80 |
| | Exp. [17] | | 50930.65 | | 1460.57 | 13.829 | 2.6 | 1.4548 | 1.824 |
| | Cal. [28] | 26616.29 | 50021.28 | 1.294 | 1442.2 | 13.6 | | 1.438 | 1.79 |
| | Cal. [58] | 29525[b] | 49938[b] | 1.2895[b] | 1449[b] | | | | |
| | Cal. [59] | 30246.81[c] | 50373[c] | 1.2867[c] | 1460.7[c] | | | | |
| | Cal. [35] | 29536.82 | 50381.40 | 1.2859 | 1463.71 | 13.8361 | | 1.45596 | 1.812 |
| $B^3\Pi_g$ | This paper | 39532.20 | 59738.83 | 1.2128 | 1732.93 | 14.1594 | −2.482 | 1.63679 | 1.779 |
| | Exp. [11] | 39494.14 | 59306.81 | 1.2126 | 1733.39 | 14.1221 | −5.688 | 1.63745 | 1.791 |
| | Exp. [12] | | 59619.35 | 1.2126 | 1733.39 | 14.122 | | 1.63745 | 1.791 |
| | Exp. [17] | 39491.31 | 59618.86 | 1.2124 | 1733.99 | 14.3919 | | 1.63788 | 1.8129 |
| | Cal. [28] | 35327.07 | 61716.31 | 1.216 | 1730.4 | 14.5 | | 1.627 | 1.82 |
| | Cal. [58] | 39376[b] | 59325[b] | 1.2148[b] | 1724[b] | | | | |
| | Cal. [59] | 39571.28[c] | 59865[c] | 1.2132[c] | 1733.8[c] | | | | |
| | Cal. [35] | 39437.27 | 59867.28 | 1.2119 | 1729.38 | 14.1099 | | 1.63665 | 1.7163 |
| $W^3\Delta_u$ | This paper | 39288.52 | 59750.11 | 1.2796 | 1508.06 | 12.4937 | 1.606 | 1.47042 | 1.696 |
| | Exp. [11,61] | 39305.8 | 59380 | | 1501.4 | 11.6 | | | |
| | Exp. [12,62] | | 59808 | | 1501.4 | 11.6 | | | |
| | Exp. [20] | 39304.99 | 59805.18 | 1.2797 | 1506.49 | 12.5469 | | 1.47027 | 1.7061 |
| | Cal. [28] | 36698.21 | 60264.52 | 1.285 | 1497.1 | 12.1 | | 1.457 | 1.66 |
| | Cal. [58] | 39225[b] | 59475[b] | 1.2828[b] | 1495[b] | | | | |
| | Cal. [59] | 39518.82[c] | 59919[c] | 1.2798[c] | 1507.6[c] | | | | |
| | Cal. [35] | 39290.48 | 59985.85 | 1.2796 | 1507.67 | 12.5694 | | 1.47043 | 1.7035 |
| $B'^3\Sigma_u^-$ | This paper | 42510.80 | 66268.90 | 1.2783 | 1518.20 | 11.9638 | 1.786 | 1.47307 | 1.647 |
| | Exp. [11] | 42456.54 | 65852.35 | 1.2784 | 1516.88 | 12.1811 | | 1.47323 | 1.6656 |
| | Exp. [12] | | 66272.47 | 1.2784 | 1516.88 | 12.181 | | 1.4733 | 1.666 |
| | Exp. [20] | | | 1.2784 | 1516.81 | 12.115 | 3.2 | 1.47314 | 1.667 |
| | Cal. [28] | 40811.64 | 67039.57 | 1.284 | 1510.1 | 11.6 | | 1.461 | 1.62 |
| | Cal. [58] | 42630[b] | 66045[b] | 1.2812[b] | 1507[b] | | | | |
| | Cal. [59] | 42663.11 | 66508 | 1.2784 | 1518.8 | | | | |
| | Cal. [35] | 42479.60 | 66494.74 | 1.2783 | 1518.32 | 12.1181 | | 1.47342 | 1.6640 |
| $w^1\Delta_u$ | This paper | 46273.82 | 72059.74 | 1.2684 | 1562.11 | 12.0017 | 4.146 | 1.49672 | 1.63 |
| | Exp. [11,63] | 46241.86 | 71698.49 | 1.2688 | 1559.50 | 12.0078 | 4.542 | 1.49554 | 1.62 |
| | Exp. [12] | | 72097.4 | 1.268 | 1559.26 | 11.63 | | 1.498 | 1.66 |
| | Exp. [23] | | | 1.2685 | 1559.34 | 11.929 | 3.49 | 1.49626 | 1.638 |
| | Cal. [57] | 42424.85[a] | 71928.49[a] | 1.2877[a] | 1546[a] | | | | |
| | Cal. [58] | 45027[b] | 71694[b] | 1.2710[b] | 1551[b] | | | | |
| | Cal. [59] | 46153.67[c] | 72097[c] | 1.2683[c] | 1561.2[c] | | | | |
| | Cal. [33] | | 73494 | 1.271 | 1559.1 | 12.39 | 15.4 | 1.4910 | 1.60 |
| $1^1\Gamma_g$ | This paper | 14758.27 | 102590.25 | 1.6073 | 801.45 | 9.5200 | 18.302 | 0.92971 | 0.931 |
| | Cal. [26] | 17582.88 | 100738.61 | 1.60 | 856.2 | 9.7 | | 0.94 | 1.1 |
| | Cal. [33] | | 102993 | 1.608 | 816.5 | 9.35 | | 0.9305 | 1.23 |
| $2^3\Sigma_u^+$ | This paper | 18000.63 | 102792.94 | 1.1168 | 2165.11 | 12.8504 | −66.907 | 1.92937 | 1.764 |
| $a^1\Pi_g$ | This paper | 48988.61 | 69387.48 | 1.2211 | 1694.74 | 14.1178 | 1.514 | 1.61479 | 1.782 |
| | Exp. [11,64] | 49055.62 | 68951.21 | 1.2203 | 1694.19 | 13.9480 | | 1.61698 | 1.7984 |
| | Exp. [12,65] | | 69283.06 | 1.2203 | 1694.21 | 13.9491 | | 1.6169 | 1.793 |
| | Exp. [23] | | | 1.2204 | 1694.20 | 13.956 | 1.02 | 1.61675 | 1.788 |
| | Cal. [57] | 46054.24[a] | 68307.07[a] | 1.2425[a] | 1686[a] | | | | |
| | Cal. [58] | 48655[b] | 69067[b] | 1.2232[b] | 1679[b] | | | | |
| | Cal. [59] | 48864.27[c] | 69386[c] | 1.2215[c] | 1692.2[c] | | | | |
| | Cal. [33] | | 69971 | 1.225 | 1687.5 | 13.91 | 1.83 | 1.6034 | 1.78 |
| $a'^1\Sigma_u^-$ | This paper | 50294.32 | 68072.83 | 1.2751 | 1533.33 | 12.0093 | 3.320 | 1.47914 | 1.605 |
| | Exp. [11] | 50186.29 | 67739.29 | 1.2754 | 1530.27 | 12.0778 | 4.1534 | 1.48012 | 1.6618 |
| | Exp. [12,66] | | 68152.66 | 1.2755 | 1530.25 | 12.0747 | | 1.4799 | 1.657 |
| | Cal. [57] | 46376.86[a] | 68008.64[a] | 1.2949[a] | 1512[a] | | | | |
| | Cal. [58] | 50160[b] | 67567[b] | 1.2781[b] | 1521[b] | | | | |
| | Cal. [59] | 50221.32[c] | 68151[c] | 1.2754[c] | 1529.3[c] | | | | |
| | Cal. [33] | | 69032 | 1.278 | 1523.6 | 11.91 | 2.8 | 1.4725 | 1.66 |
| $C^3\Pi_u$ | This paper | 9957.73 | 88909.33 | 1.1480 | 2070.52 | 28.42 | | 1.82943 | 2.738 |

(*continued*).

**Table 2.** Continued.

| Electronic state | | $D_e$/cm$^{-1}$ | $T_e$/cm$^{-1}$ | $R_e$/Å | $\omega_e$/cm$^{-1}$ | $\omega_e x_e$/cm$^{-1}$ | $10^2\omega_e y_e$/cm$^{-1}$ | $B_e$/cm$^{-1}$ | $10^2\alpha_e$/cm$^{-1}$ |
|---|---|---|---|---|---|---|---|---|---|
| | Exp. [11] | 9976.71 | 88977.84 | 1.1487 | 2047.18 | 28.445 | | 1.82473 | 1.8683 |
| | Exp. [12] | | 89136.88 | 1.1487 | 2047.18 | 28.445 | | 1.82473 | 1.868 |
| | Exp. [24] | | | 1.1480 | 2047.79 | 28.942 | 2.245 | 1.82682 | 2.4 |
| | Cal. [28] | | 91558.82 | 1.150 | 2078 | 29 | | 1.821 | 2.01 |
| | Cal. [58] | 9660$^b$ | 89040$^b$ | 1.1509$^b$ | 2031$^b$ | | | | |
| | Cal. [59] | 9961.02$^c$ | 89475$^c$ | 1.1486$^c$ | 2040.7$^c$ | | | | |
| C$'^3\Pi_u$ | This paper$^d$ | 3003.34 | 97898.53 | 1.5111 | | | | | |
| | Exp. [12] | | 98351 | 1.5146 | | | | | |
| | Exp. [67] | | 97563.7$^e$ | | | | | | |
| E$^3\Sigma_g^+$ | This paper | 25130.04 | 95280.55 | 1.1134 | 2228.40 | 15.3160 | 5.941 | 1.93540 | 1.265 |
| | Exp. [11] | | 95774.5 | 1.1177 | 2185 | | | 1.9273 | |
| | Exp. [12,68] | | 95858 | 1.1177 | 2185 | | | 1.9273 | |
| | Cal. [33] | | 95900 | 1.121 | 2216.3 | 12.8 | −40 | 1.914 | 3 |
| b$^1\Pi_u$ | This paper | 16274.55 | 101284.02 | 1.3322 | 661.05 | −8.0860 | −38.067 | 1.34333 | −0.495 |
| | Exp. [11] | | 100817.5 | 1.279 | | | | 1.4601 | 2.6239 |
| | Exp. [12] | 16662.33 | 101675 | 1.2841 | 634.8 | | | 1.4483 | |
| | Cal. [58] | 16384$^b$ | 101337$^b$ | 1.3248$^b$ | 517$^b$ | | | | |
| | Cal. [59] | 16281.10$^c$ | 101969$^c$ | 1.2918$^c$ | 573.6$^c$ | | | | |
| a$''^1\Sigma_g^+$ (1st well) | This paper | 7096.55 | 97880.67 | 1.1160 | 2194.95 | 5.6918 | | 1.93424 | 2.336 |
| | Cal. [33] | | 95914 | 1.105 | | | | 1.9704 | 10 |
| a$''^1\Sigma_g^+$ (2nd well) | This paper | 26867.41 | 90591.27 | 1.5601 | 844.70 | −12.4401 | −89.963 | 0.98874 | 1.024 |
| | Cal. [33] | | 90521 | 1.558 | 933.9 | −2.16 | | 0.9915 | 1.0 |
| G$^3\Delta_g$ | This paper | 9638.48 | 88581.24 | 1.6084 | 772.02 | 12.2416 | −2.67 | 0.92827 | 1.339 |
| | Exp. [11,69] | 11180 | 87100 | 1.6107 | 765.9 | 11.85 | | 0.9280 | 1.61 |
| | Exp. [12] | | 87900 | 1.6107 | 742.49 | 11.85 | | 0.9280 | 1.61 |
| | Exp. [26] | 11049.80 | 87995.05 | 1.61 | 765.9 | 13.2 | | 0.93 | 1.6 |
| | Cal. [58] | 9802$^b$ | 88898$^b$ | 1.6140$^b$ | 764$^b$ | | | | |
| | Cal. [59] | 9607.77$^c$ | 89828$^c$ | 1.6103$^c$ | 758.2$^c$ | | | | |
| | Cal. [33] | | 89721 | 1.615 | 749.6 | 11.71 | | 0.9224 | 1.67 |
| 1$^3\Sigma_g^-$ | This paper | 9943.43 | 98054.87 | 1.6095 | 769.92 | 13.0724 | 13.163 | 0.92632 | 1.272 |
| | Cal. [26] | 11614.38 | 97109.11 | 1.61 | 792 | 7.4 | | 0.93 | 0.79 |
| | Cal. [33] | | 97776 | 1.614 | 761 | 12.16 | −14 | 0.9225 | 1.6 |
| 2$^3\Sigma_g^-$ | This paper | 3630.61 | 113915.70 | 1.7714 | 497.82 | −23.691 | −1.490 | 0.77135 | 2.130 |
| | Cal. [33] | | 114580 | 1.817 | 428 | 9.27 | −81 | 0.7285 | 1.5 |
| 2$^3\Sigma_g^-$ | This paper | 3600.53 | 116050.93 | 1.7306 | 640.99 | 4.3542 | 96.978 | 0.80076 | 0.473 |

$^a$At FCI/cc-PVDZ level of theory, $^b$MR-CISD + Q/TQ, $^c$MR-ccCA-P except that Pople's correction is used instead of Davidson's correction, $^d$Only one vibrational level is calculated at 432.59 in cm$^{-1}$, $^e$given at the v = 0 level of C$'^3\Pi_u$.

internuclear distances, the predicted potential energy curve lies between that of Little and Tennyson [36] and that of Spelsberg and Meyer [45]. As shown in Figure 4, a good agreement of the b$'^1\Sigma_u^+$ state is observed, thus confirming a good description of the b$'^1\Sigma_u^+$ state in this work.

Table 2 presents the spectroscopic parameters of the electronic states for N$_2$, together with their comparisons with the available theoretical values, the experimental data of Lofthus and Krupenie [11] and of Huber and Herzberg [12] and of Roux et al. [20,23,24]. For the X$^1\Sigma_g^+$, A$^3\Sigma_u^+$, B$^3\Pi_g$, W$^3\Delta_u$, B$'^3\Sigma_u^-$, a$^1\Pi_g$, a$'^1\Sigma_u^-$ and C$^3\Pi_u$ states, the calculated and measured internuclear distances differ by less than 0.001Å, and the differences are less than 0.01Å for the other lower states, except for the b$^1\Pi_u$ state whose difference is about 0.05 Å. An excellent agreement is observed between the calculated values of the other spectroscopic parameters and those determined experimentally for the lower states. Hence, a similar accuracy is assumed for the spectroscopic parameters of higher-lying states that have not been observed
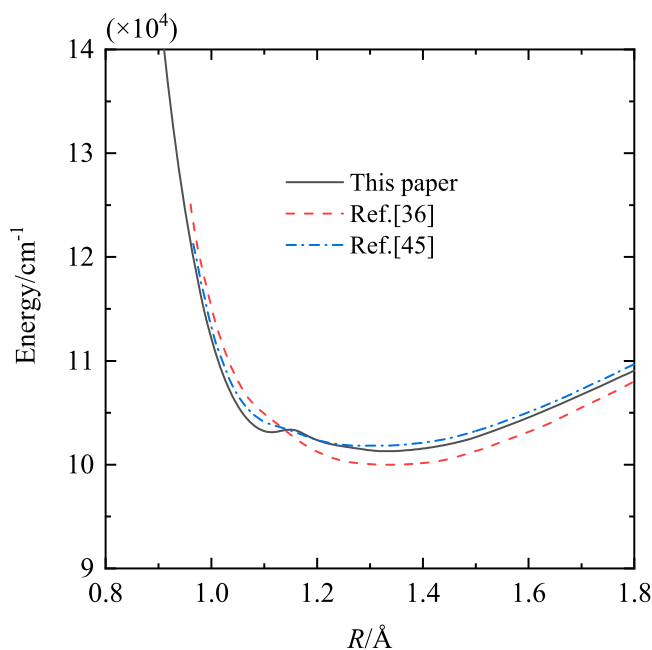


**Figure 3.** N$_2$ b$^1\Pi_u$ state compared to that of Little and Tennyson [36] and that of Spelsberg and Meyer [45].
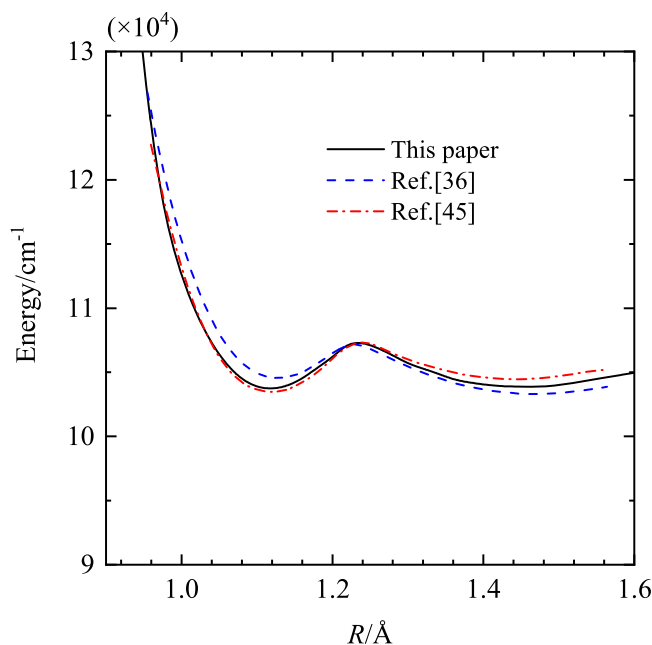
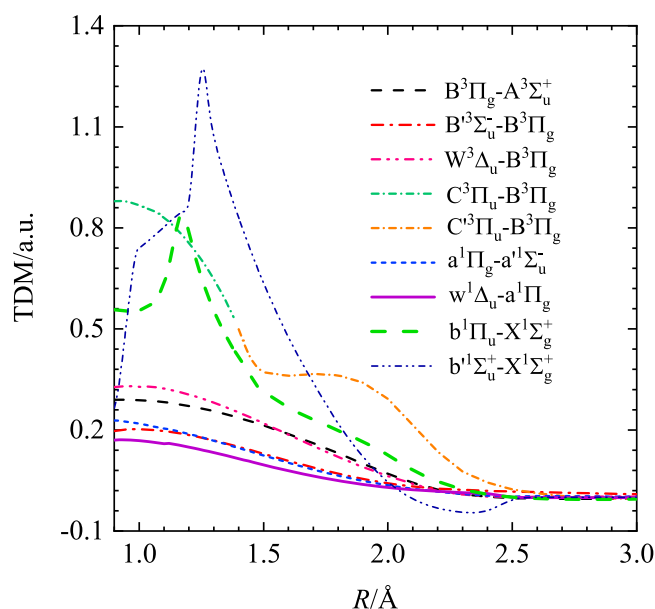**Figure 4.** $N_2$ $b'^1\Sigma_u^+$ state compared to that of Little and Tennyson [36] and that of Spelsberg and Meyer [45].



**Figure 5.** TDMs of the $B^3\Pi_g - A^3\Sigma_u^+$, $C^3\Pi_u - B^3\Pi_g$, $W^3\Delta_u - B^3\Pi_g$, $B'^3\Sigma_u^- - B^3\Pi_g$, $C'^3\Pi_u - B^3\Pi_g$, $w^1\Delta_u - a^1\Pi_g$, $a^1\Pi_g - a'^1\Sigma_u^-$, $b^1\Pi_u - X^1\Sigma_g^+$ and $b'^1\Sigma_u^+ - X^1\Sigma_g^+$ band transition systems of $N_2$ calculated at the icMRCI/AV6Z level of theory.

experimentally. It should be noted that the calculated vibrational levels and internal rotation constants of the $X^1\Sigma_g^+$, $A^3\Sigma_u^+$, $B^3\Pi_g$, $W^3\Delta_u$, $B'^3\Sigma_u^-$, $C^3\Pi_u$, $w^1\Delta_u$, $a^1\Pi_g$ and $a'^1\Sigma_u^-$ states are given and compared with available experimental values in the Supplementary Material. An overall agreement can be observed for these states.

## B. Transition dipole moments, radiative transition probabilities and radiative lifetimes

As mentioned in the introduction, the transition properties of the $B^3\Pi_g - A^3\Sigma_u^+$, $C^3\Pi_u - B^3\Pi_g$ and $W^3\Delta_u - B^3\Pi_g$ band systems were extensively studied experimentally, and the $w^1\Delta_u - a^1\Pi_g$, $a^1\Pi_g - a'^1\Sigma_u^-$, $B'^3\Sigma_u^- - B^3\Pi_g$, $C'^3\Pi_u - B^3\Pi_g$ transitions were also observed in previous experiments. Theoretically, Werner et al. carried out accurate ab initio calculations of the transition properties for the $B^3\Pi_g - A^3\Sigma_u^+$, $C^3\Pi_u - B^3\Pi_g$, $W^3\Delta_u - B^3\Pi_g$ and $B'^3\Sigma_u^- - B^3\Pi_g$ band systems of $N_2$. However, the transition properties of $N_2$ was less reported since then. For brevity, the TDMs of the $B^3\Pi_g - A^3\Sigma_u^+$, $C^3\Pi_u - B^3\Pi_g$, $W^3\Delta_u - B^3\Pi_g$, $B'^3\Sigma_u^- - B^3\Pi_g$, $C'^3\Pi_u - B^3\Pi_g$, $w^1\Delta_u - a^1\Pi_g$, $a^1\Pi_g - a'^1\Sigma_u^-$, $b^1\Pi_u - X^1\Sigma_g^+$ and $b'^1\Sigma_u^+ - X^1\Sigma_g^+$ systems are given in Figure 5, and the radiative transition probabilities of these 9 band transition systems are presented in the Supplementary Material. Moreover, radiative lifetimes of the $B^3\Pi_g$, $C^3\Pi_u$ and $W^3\Delta_u$ states are shown in Figure 6 and compared with the available experimental and theoretical values.

As shown in Figure 6(a), the vibrational radiative lifetimes of $N_2$ $B^3\Pi_g$ state are given and compared with the theoretical and experimental results. A good agreement is observed between the theoretical values of the vibrational radiative lifetimes from Ref. [71] and Ref. [28]. Our calculated vibrational radiative lifetimes are lower than previous calculated results of Refs. [28,71]. However, the radiative lifetimes for $v' = 5$–12 are in excellent agreement with the experimental results of Refs. [14,72]. For the vibrational levels of $v' = 0$–4, the radiative lifetimes are closer to the experimental results of Ref. [14] than the theoretical values calculated by Chauveau et al. [71] and Werner et al.[28]. For the $C^3\Pi_u$ state, the vibrational radiative lifetimes are shown in Figure 6(b), together with the theoretical values of Refs. [28,71] and the experimental results of Refs. [73–75]. As shown, the experimental vibrational radiative lifetimes exhibit a quite large dispersion. For $v' = 0$, our calculated radiative lifetime is within the error bars of both the experimental value of Ref. [74] and Ref. [75]. And the calculated radiative lifetime of $v' = 4$ is within the allowable error range of the experimental results of Refs. [73,75]. Figure 6(c) shows the vibrational radiative lifetimes of $N_2$ $W^3\Delta_u$ electronic state from this work and other references. Large differences are observed between our calculated vibrational radiative lifetimes and those computed by Werner et al. [28]. Yet the radiative lifetimes of $v' = 3$–7 are in good agreement with the only experimental values [62] that we can be found in the literature. For $v' = 1$ and 2, the
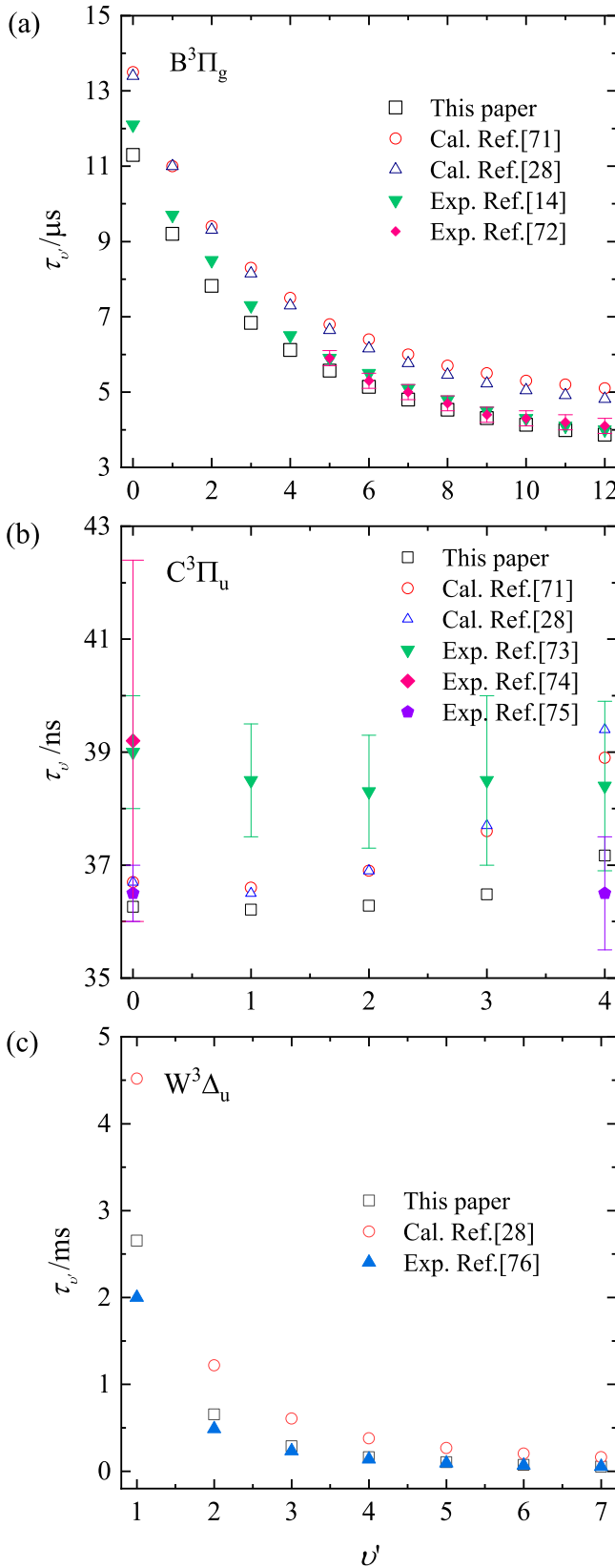
**Figure 6.** Comparisons of the vibrational radiative lifetimes for **(a)** $N_2$ $B^3\Pi_g$ electronic state with the theoretical results of Refs. [28,71] and the experimental values of Refs. [14,72], **(b)** $N_2$ $C^3\Pi_u$ electronic state with the theoretical results of Refs. [28,71] and the experimental values of Refs. [73–75], (c) $N_2$ $W^3\Delta_u$ electronic state with the theoretical results of Ref. [28] and the experimental values of Ref. [62].

radiative lifetimes are slightly higher than the experimental values of Ref. [62].

Of particular interest are some less studied radiative transition systems, which will be elaborated below. The $E^3\Sigma_g^+ - A^3\Sigma_u^+$ transition was first observed by Kaplan [76] and Herman [77], later confirmed by many theoretical and experimental researches [33,68,78,79]. Nevertheless, there remains uncertainties relating to this band transition system due to the metastability of the $E^3\Sigma_g^+$ state and the spin-orbital conversions from the adjacent electronic states. Hochlaf et al. [33] investigated the spin-orbital integrals between the $E^3\Sigma_g^+$ state and the adjacent $1^3\Sigma_g^-$, $2^3\Sigma_g^-$, $B^3\Pi_g$, $2^3\Pi_g$, $3^3\Pi_g$, $2^5\Pi_g$, $3^5\Pi_g$ states and pointed out that the measured radiative lifetime for the $E^3\Sigma_g^+$ state of $270 \pm 100\mu s$ by Freund [68] is relatively long due to the perturbation by the $1^3\Sigma_g^-$ state. However, transition properties of the $E^3\Sigma_g^+ - A^3\Sigma_u^+$ system has not been fully understood until now. The calculated TDMs for this band transition system are given in Table 3, together with those of the $E^3\Sigma_g^+ - C^3\Pi_u$ and $2^3\Sigma_u^+ - E^3\Sigma_g^+$ systems. Our calculations indicate that the $2^3\Sigma_u^+$ state is lying slightly higher than the $E^3\Sigma_g^+$ state. And the $2^3\Sigma_u^+ - E^3\Sigma_g^+$ emission is predicted to be relatively strong with large transition probabilities of $6.515 \times 10^6$, $7.173 \times 10^6$, $7.900 \times 10^6$ and $8.816 \times 10^6 \, sec^{-1}$ for 0-0, 1-1, 2–2 and 3–3 vibrational transition bands, respectively.

The presence of the $1^3\Sigma_g^-$ and $2^3\Sigma_g^-$ electronic states was confirmed by Hochlaf et al. [33], who also presented the potential energy curves of these two electronic states. The TDMs of the $1^3\Sigma_g^- - C'^3\Pi_u$, $2^3\Pi_u - 1^3\Sigma_g^-$ and $3^3\Pi_u - 1^3\Sigma_g^-$ systems are presented in Figure 7, together with those of the $2^3\Sigma_g^- - C'^3\Pi_u$, $2^3\Sigma_g^- - 2^3\Pi_u$, $2^3\Sigma_g^- - 3^3\Pi_u$ and $1^3\Sigma_g^- - B'^3\Sigma_u^-$ systems. For the internuclear distance $R = 1.62\text{Å}$, the calculated TDMs of the $C'^3\Pi_u - 1^3\Sigma_g^-$, $2^3\Pi_u - 1^3\Sigma_g^-$ and $3^3\Pi_u - 1^3\Sigma_g^-$ transition systems are 0.201, 0.113, 0.346 Debye, respectively, which are slightly smaller than the values given by Hochlaf et al. [33]. Such deviations are mostly due to the CV correlation energy correction and the larger basis set adopted in this work. As shown in Figure 1, the $1^3\Sigma_g^-$ and $2^3\Sigma_g^-$ states are intersected with the $^3\Pi_u$ states, which may contribute to the radiative transitions or mutual couplings between the $^3\Sigma_g^-$ states ($1^3\Sigma_g^-$ and $2^3\Sigma_g^-$ states) and the $^3\Pi_u$ states. In order to investigate such radiative transition properties, radiative transition probabilities between the $^3\Sigma_g^-$ states ($1^3\Sigma_g^-$ and $2^3\Sigma_g^-$ states) and the $^3\Pi_u$ states are calculated. Radiative transitions from the $1^3\Sigma_g^-$ and $2^3\Sigma_g^-$ states to $C'^3\Pi_u$ state are found to be relatively strong and their Einstein coefficients are given in Table 4. In

**Table 3.** TDMs of the $E^3\Sigma_g^+ - A^3\Sigma_u^+$, $E^3\Sigma_g^+ - C^3\Pi_u$, $2^3\Sigma_u^+ - E^3\Sigma_g^+$, $2^3\Sigma_u^+ - B^3\Pi_g$ and $b^1\Pi_u - a''^1\Sigma_g^+$ (1st well) band transition systems of N$_2$ calculated at the icMRCI/AV6Z level of theory.

| $E^3\Sigma_g^+ - A^3\Sigma_u^+$ | | $E^3\Sigma_g^+ - C^3\Pi_u$ | | $2^3\Sigma_u^+ - E^3\Sigma_g^+$ | | $2^3\Sigma_u^+ - B^3\Pi_g$ | | $b^1\Pi_u - a''^1\Sigma_g^+$ (1st well) | |
|---|---|---|---|---|---|---|---|---|---|
| R/Å | TDM/a.u. | R/Å | TDM/a.u. | R/Å | TDM/a.u. | R/Å | TDM/a.u. | R/Å | TDM/a.u. |
| 0.94 | 0.2267 | 1.02 | 0.0903 | 0.94 | 2.5209 | 0.94 | 0.3200 | 0.80 | 3.0524 |
| 0.98 | 0.1073 | 1.04 | 0.0963 | 0.96 | 2.5662 | 0.98 | 0.3111 | 0.84 | 3.0526 |
| 1.02 | 0.0665 | 1.06 | 0.0999 | 0.98 | 2.6009 | 1.00 | 0.3029 | 0.88 | 3.0508 |
| 1.06 | 0.0467 | 1.08 | 0.1019 | 1.00 | 2.6291 | 1.02 | 0.2943 | 0.92 | 3.0475 |
| 1.10 | 0.0352 | 1.10 | 0.1026 | 1.02 | 2.6528 | 1.04 | 0.2858 | 0.94 | 3.0430 |
| 1.14 | 0.0273 | 1.12 | 0.1025 | 1.04 | 2.6731 | 1.06 | 0.2776 | 0.96 | 3.0376 |
| 1.18 | 0.0213 | 1.14 | 0.1016 | 1.06 | 2.6910 | 1.08 | 0.2699 | 0.98 | 3.0313 |
| 1.22 | 0.0165 | 1.16 | 0.1001 | 1.08 | 2.7070 | 1.10 | 0.2628 | 1.00 | 3.0243 |
| 1.26 | 0.0165 | 1.18 | 0.0982 | 1.10 | 2.7216 | 1.12 | 0.2568 | 1.02 | 3.0178 |
| 1.28 | 0.0171 | 1.20 | 0.0959 | 1.12 | 2.7352 | 1.14 | 0.2514 | 1.04 | 3.0178 |
| 1.30 | 0.0175 | 1.22 | 0.0933 | 1.14 | 2.7481 | 1.16 | 0.2515 | 1.06 | 3.0173 |
| 1.32 | 0.0177 | 1.24 | 0.0908 | 1.16 | 2.7498 | 1.18 | 0.2458 | 1.08 | 3.0064 |
| 1.34 | 0.0177 | 1.26 | 0.0883 | 1.18 | 2.7555 | 1.20 | 0.2402 | 1.10 | 3.0021 |
| 1.36 | 0.0171 | 1.28 | 0.0859 | 1.20 | 2.7545 | 1.22 | 0.2347 | 1.12 | 2.9812 |
| 1.38 | 0.0153 | 1.30 | 0.0893 | 1.22 | 2.7386 | 1.24 | 0.2290 | 1.16 | 2.1937 |
| 1.40 | 0.0105 | 1.32 | 0.0935 | 1.24 | 2.6334 | 1.26 | 0.2229 | 1.20 | 1.0852 |
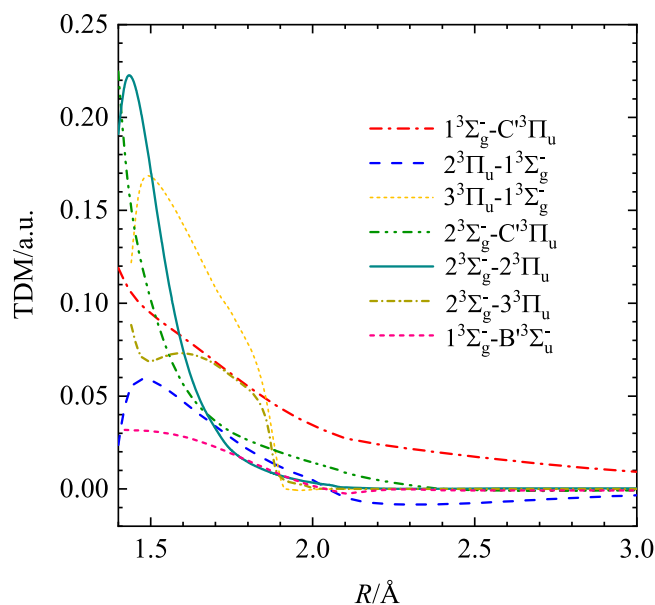


**Figure 7.** TDMs of the $1^3\Sigma_g^- - C'^3\Pi_u$, $2^3\Pi_u - 1^3\Sigma_g^-$, $3^3\Pi_u - 1^3\Sigma_g^-$, $2^3\Sigma_g^- - C'^3\Pi_u$, $2^3\Sigma_g^- - 2^3\Pi_u$, $2^3\Sigma_g^- - 3^3\Pi_u$ and $1^3\Sigma_g^- - B'^3\Sigma_u^-$ band transition systems of N$_2$ calculated at the icMRCI/AV6Z level of theory.

addition, the $1^3\Sigma_g^-$ and $2^3\Sigma_g^-$ states can also emit to the lower $B'^3\Sigma_u^-$ state. Transitions from the $2^3\Sigma_g^-$ state to the $B'^3\Sigma_u^-$ state are most likely occurring according to our calculated Einstein coefficients, which are given in Table 5. The $1^3\Sigma_g^- - B'^3\Sigma_u^-$ transition is relatively weak.

The $2^3\Delta_g$ state was predicted by Michels [26] to converge to the $N(^2D_u) + N(^2D_u)$ dissociation limit with a shallow potential well. This electronic state is confirmed by our calculations and located at about $116050\,\mathrm{cm}^{-1}$ with a potential well of $3600.53\,\mathrm{cm}^{-1}$. The equilibrium internuclear distance is 1.7306Å. By solving the Schrödinger equation over the obtained potential energy curve of the $2^3\Delta_g$ state, we determine 6 vibrational levels at 320.56, 953.93, 1591.03, 2231.55, 2856.90 and $3527.95\,\mathrm{cm}^{-1}$, respectively. According to the selection rules of radiative transitions, the $2^3\Delta_g$ state can decay to the $W^3\Delta_u$, $^3\Pi_u$ and $H^3\Phi_u$ states. Our calculations indicate that the transitions of the $2^3\Delta_g$ state to the $^3\Pi_u$ states are relatively weak. The TDMs of the $2^3\Delta_g - W^3\Delta_u$ and $2^3\Delta_g - H^3\Phi_u$ systems are shown in Figure 8 and used to calculate the radiative transition probabilities, which are given in Table 6.

The first-positive ($B^3\Pi_g - A^3\Sigma_u^+$) system is one of the most important band transition systems in N$_2$ spectrum and has been extensively studied so far. The $2^3\Sigma_u^+$ state is less studied although it has the same symmetry as $A^3\Sigma_u^+$. In our work, the $2^3\Sigma_u^+$ state is found to have a potential well above the dissociation limit, which enable to carry

**Table 4.** Einstein coefficients ($s^{-1}$) for the $1\,^3\Sigma_g^- - C'\,^3\Pi_u$, $2\,^3\Sigma_g^- - C'\,^3\Pi_u$ and $b\,^1\Pi_u - a''\,^1\Sigma_g^+$ (1st well) band transition systems of $N_2$.
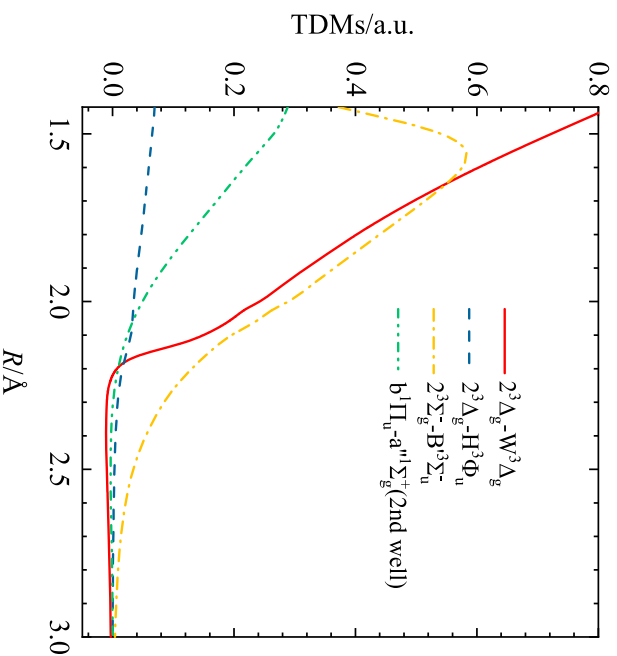
| Transition system | $v''$ | $v'$ | | | | | | | | | | | |
|---|---|---|---|---|---|---|---|---|---|---|---|---|---|
| | | 0 | 1 | 2 | 3 | 4 | 5 | 6 | 7 | 8 | 9 | 10 | 11 |
| $1\,^3\Sigma_g^- - C'\,^3\Pi_u$ | 0 | $3.000 \times 10^{-3}$ | $7.098 \times 10^1$ | $4.612 \times 10^2$ | $3.719 \times 10^2$ | $9.860 \times 10^{-2}$ | $4.773 \times 10^2$ | $1.037 \times 10^3$ | $1.162 \times 10^3$ | $1.457 \times 10^3$ | $2.845 \times 10^3$ | $6.376 \times 10^3$ | $1.160 \times 10^4$ |
| $2\,^3\Sigma_g^- - C'\,^3\Pi_u$ | 0 | $6.038 \times 10^2$ | $3.424 \times 10^3$ | $1.035 \times 10^4$ | $2.498 \times 10^4$ | $4.299 \times 10^4$ | $6.238 \times 10^4$ | $7.595 \times 10^4$ | | | | | |
| $b\,^1\Pi_u - a''\,^1\Sigma_g^+$ (1st well) | 0 | $1.235 \times 10^3$ | $4.211 \times 10^4$ | $4.800 \times 10^5$ | $2.936 \times 10^6$ | $5.701 \times 10^6$ | $3.141 \times 10^6$ | $1.134 \times 10^6$ | $2.121 \times 10^5$ | $4.630 \times 10^3$ | $1.754 \times 10^5$ | $2.706 \times 10^5$ | $1.811 \times 10^5$ |
| | 1 | $5.708 \times 10^2$ | $1.283 \times 10^4$ | $5.500 \times 10^4$ | $1.131 \times 10^4$ | $3.876 \times 10^5$ | $2.022 \times 10^6$ | $4.169 \times 10^6$ | $6.155 \times 10^6$ | $6.373 \times 10^6$ | $4.190 \times 10^6$ | $1.518 \times 10^6$ | $1.694 \times 10^5$ |
| | 2 | $8.102 \times 10^1$ | $2.780 \times 10^3$ | $4.111 \times 10^3$ | $4.403 \times 10^3$ | $5.824 \times 10^4$ | $1.225 \times 10^4$ | $1.227 \times 10^5$ | $1.251 \times 10^6$ | $4.216 \times 10^6$ | $7.799 \times 10^6$ | $9.257 \times 10^6$ | $8.032 \times 10^6$ |

**Table 4.** Einstein coefficients ($s^{-1}$) for the $1\,^3\Sigma_g^- - C'\,^3\Pi_u$ and $b\,^1\Pi_u - a''\,^1\Sigma_g^+$ (1st well) band transition systems of $N_2$ (continued).

| Transition system | $v''$ | $v'$ | | | | | | | | | | |
|---|---|---|---|---|---|---|---|---|---|---|---|---|
| | | 12 | 13 | 14 | 15 | 16 | 17 | 18 | 19 | 20 | 21 | 22 | 23 |
| $1\,^3\Sigma_g^- - C'\,^3\Pi_u$ | 0 | $1.721 \times 10^4$ | $2.043 \times 10^4$ | $2.015 \times 10^4$ | $1.780 \times 10^4$ | $1.492 \times 10^4$ | $1.168 \times 10^4$ | $9.265 \times 10^3$ | $7.278 \times 10^3$ | $5.551 \times 10^3$ | $1.140 \times 10^2$ | | |
| $b\,^1\Pi_u - a''\,^1\Sigma_g^+$ (1st well) | 0 | $5.267 \times 10^4$ | $1.292 \times 10^2$ | $2.823 \times 10^4$ | $7.304 \times 10^4$ | $8.219 \times 10^4$ | $5.484 \times 10^4$ | $2.026 \times 10^4$ | $1.673 \times 10^3$ | $2.268 \times 10^3$ | $1.652 \times 10^3$ | $2.806 \times 10^3$ | $3.128 \times 10^3$ |
| | 1 | $5.398 \times 10^4$ | $3.957 \times 10^5$ | $2.833 \times 10^5$ | $4.565 \times 10^5$ | $1.995 \times 10^5$ | $2.889 \times 10^4$ | $6.291 \times 10^3$ | $6.641 \times 10^4$ | $1.241 \times 10^5$ | $1.635 \times 10^4$ | $1.342 \times 10^4$ | $8.837 \times 10^3$ |
| | 2 | $5.275 \times 10^6$ | $2.415 \times 10^6$ | $5.542 \times 10^5$ | $5.818 \times 10^2$ | $2.417 \times 10^5$ | $5.787 \times 10^5$ | $6.516 \times 10^5$ | $4.817 \times 10^5$ | $2.449 \times 10^5$ | $7.663 \times 10^3$ | $6.285 \times 10^2$ | $4.473 \times 10^2$ |

**Table 5.** Einstein coefficients (s$^{-1}$) for the $2^3\Sigma$- g-B$'^3\Sigma$- u band transition systems of N$_2$.

| | | | | | | $v'$ | | | | | | | |
|---|---|---|---|---|---|---|---|---|---|---|---|---|---|
| $v''$ | 0 | 1 | 2 | 3 | 4 | 5 | 6 | 7 | 8 | 9 | 10 | 11 | 12 |
| 0 | $4.961 \times 10^{-2}$ | $1.181 \times 10^{0}$ | $1.374 \times 10^{1}$ | $1.057 \times 10^{2}$ | $6.046 \times 10^{2}$ | $2.721 \times 10^{3}$ | $9.969 \times 10^{3}$ | $3.044 \times 10^{4}$ | $7.882 \times 10^{4}$ | $1.756 \times 10^{5}$ | $3.397 \times 10^{5}$ | $5.749 \times 10^{5}$ | $8.562 \times 10^{5}$ |
| 1 | $8.513 \times 10^{-1}$ | $1.843 \times 10^{1}$ | $1.924 \times 10^{2}$ | $1.318 \times 10^{3}$ | $6.666 \times 10^{3}$ | $2.634 \times 10^{4}$ | $8.383 \times 10^{4}$ | $2.192 \times 10^{5}$ | $4.772 \times 10^{5}$ | $8.729 \times 10^{5}$ | $1.344 \times 10^{6}$ | $1.735 \times 10^{6}$ | $1.855 \times 10^{6}$ |
| 2 | $7.233 \times 10^{0}$ | $1.426 \times 10^{2}$ | $1.333 \times 10^{3}$ | $8.096 \times 10^{3}$ | $3.604 \times 10^{4}$ | $1.242 \times 10^{5}$ | $3.400 \times 10^{5}$ | $7.507 \times 10^{5}$ | $1.347 \times 10^{6}$ | $1.959 \times 10^{6}$ | $2.275 \times 10^{6}$ | $2.034 \times 10^{6}$ | $1.286 \times 10^{6}$ |
| 3 | $4.664 \times 10^{1}$ | $8.390 \times 10^{2}$ | $7.008 \times 10^{3}$ | $3.752 \times 10^{4}$ | $1.458 \times 10^{5}$ | $4.337 \times 10^{5}$ | $1.007 \times 10^{6}$ | $1.839 \times 10^{6}$ | $2.628 \times 10^{6}$ | $2.871 \times 10^{6}$ | $2.249 \times 10^{6}$ | $1.066 \times 10^{6}$ | $1.458 \times 10^{5}$ |
| 4 | $2.057 \times 10^{2}$ | $3.382 \times 10^{3}$ | $2.517 \times 10^{4}$ | $1.180 \times 10^{5}$ | $3.966 \times 10^{5}$ | $1.004 \times 10^{6}$ | $1.939 \times 10^{6}$ | $2.831 \times 10^{6}$ | $3.041 \times 10^{6}$ | $2.215 \times 10^{6}$ | $8.490 \times 10^{5}$ | $2.883 \times 10^{4}$ | $2.944 \times 10^{5}$ |
| 5 | $6.548 \times 10^{2}$ | $9.967 \times 10^{3}$ | $6.692 \times 10^{4}$ | $2.775 \times 10^{5}$ | $8.120 \times 10^{5}$ | $1.758 \times 10^{6}$ | $2.815 \times 10^{6}$ | $3.231 \times 10^{6}$ | $2.458 \times 10^{6}$ | $9.658 \times 10^{5}$ | $3.125 \times 10^{4}$ | $3.552 \times 10^{5}$ | $1.111 \times 10^{6}$ |
| 6 | $1.601 \times 10^{3}$ | $2.275 \times 10^{4}$ | $1.387 \times 10^{5}$ | $5.101 \times 10^{5}$ | $1.300 \times 10^{6}$ | $2.394 \times 10^{6}$ | $3.128 \times 10^{6}$ | $2.692 \times 10^{6}$ | $1.243 \times 10^{6}$ | $9.743 \times 10^{4}$ | $2.579 \times 10^{5}$ | $1.076 \times 10^{6}$ | $1.121 \times 10^{6}$ |
| 7 | $3.226 \times 10^{3}$ | $4.326 \times 10^{4}$ | $2.420 \times 10^{5}$ | $7.979 \times 10^{5}$ | $1.783 \times 10^{6}$ | $2.800 \times 10^{6}$ | $2.950 \times 10^{6}$ | $1.789 \times 10^{6}$ | $3.439 \times 10^{5}$ | $8.124 \times 10^{4}$ | $8.900 \times 10^{5}$ | $1.246 \times 10^{6}$ | $5.434 \times 10^{5}$ |
| 8 | $4.035 \times 10^{3}$ | $5.180 \times 10^{4}$ | $2.710 \times 10^{5}$ | $8.165 \times 10^{5}$ | $1.632 \times 10^{6}$ | $2.226 \times 10^{6}$ | $1.909 \times 10^{6}$ | $7.692 \times 10^{5}$ | $1.302 \times 10^{4}$ | $3.664 \times 10^{5}$ | $9.568 \times 10^{5}$ | $7.217 \times 10^{5}$ | $8.949 \times 10^{4}$ |
| 9 | $3.122 \times 10^{2}$ | $3.906 \times 10^{4}$ | $1.960 \times 10^{5}$ | $5.580 \times 10^{5}$ | $1.037 \times 10^{6}$ | $1.285 \times 10^{6}$ | $9.461 \times 10^{5}$ | $2.617 \times 10^{5}$ | $1.013 \times 10^{4}$ | $3.604 \times 10^{5}$ | $5.885 \times 10^{5}$ | $2.903 \times 10^{5}$ | $2.185 \times 10^{3}$ |
| 10 | $2.247 \times 10^{3}$ | $2.772 \times 10^{4}$ | $1.359 \times 10^{5}$ | $3.745 \times 10^{5}$ | $6.665 \times 10^{5}$ | $7.787 \times 10^{5}$ | $5.194 \times 10^{5}$ | $1.066 \times 10^{5}$ | $2.622 \times 10^{4}$ | $2.753 \times 10^{5}$ | $3.579 \times 10^{5}$ | $1.316 \times 10^{5}$ | $2.159 \times 10^{3}$ |
| 11 | $1.882 \times 10^{3}$ | $2.303 \times 10^{4}$ | $1.114 \times 10^{5}$ | $3.009 \times 10^{5}$ | $5.215 \times 10^{5}$ | $5.873 \times 10^{5}$ | $3.670 \times 10^{5}$ | $5.984 \times 10^{4}$ | $3.426 \times 10^{4}$ | $2.350 \times 10^{5}$ | $2.678 \times 10^{5}$ | $7.985 \times 10^{4}$ | $7.208 \times 10^{3}$ |
| 12 | $1.343 \times 10^{3}$ | $1.635 \times 10^{4}$ | $7.838 \times 10^{4}$ | $2.090 \times 10^{5}$ | $3.558 \times 10^{5}$ | $3.907 \times 10^{5}$ | $2.331 \times 10^{5}$ | $3.157 \times 10^{4}$ | $3.087 \times 10^{4}$ | $1.691 \times 10^{5}$ | $1.766 \times 10^{5}$ | $4.484 \times 10^{4}$ | $8.872 \times 10^{3}$ |



**Figure 8.** TDMs of the $2^3\Delta_g - W^3\Delta_u$, $2^3\Delta_g - H^3\Phi_u$, $2^3\Sigma_g^- - B^3\Sigma_u^-$ and b$^1\Pi_u$ − a$''^1\Sigma_g^+$ (2nd well) band transition systems of N$_2$ calculated at the icMRCI/AV6Z level of theory.

9 vibrational levels. Just as B$^3\Pi_g$ − A$^3\Sigma_u^+$ transition system, the $2^3\Sigma_u^+$ state is expected to undergo radiative transitions to the B$^3\Pi_g$ state. We calculate the TDMs of the $2^3\Sigma_u^+$ − B$^3\Pi_g$ band transition system (given in Table 3), which are then adopted to compute the radiative transition probabilities. Large Einstein coefficients (shown in Table 7) are obtained, which means that this band transition system is most likely to observe experimentally.

The b$^1\Pi_u$ state was known for the Birge-Hopfield I (b$^1\Pi_u$ − X$^1\Sigma_g^+$) system measured by Carroll and Collins [80] and later investigated by James et al. [81] through the measurement of the electron impact induced fluorescence spectrum of N$_2$. The a$''^1\Sigma_g^+$ state was first observed by Dressler and Lutz (a$''^1\Sigma_g^+$ − X$^1\Sigma_g^+$) system first observed by Dressler and Lutz [82,83] in an absorption spectrum of N$_2$ at pressures from 1–10 kPa. About forty years later, in the work of Hochlaf et al. [33], this state was presented with a double-well potential energy curve, which is confirmed by our calculations. According to the selection rules of radiative transition, the transition of the b$^1\Pi_u$ state to the a$''^1\Sigma_g^+$ state is allowed, but is less studied. As such, the TDMs of the b$^1\Pi_u$ − a$''^1\Sigma_g^+$ (1st well) system are calculated and presented in Table 3 and the TDMs of the b$^1\Pi_u$ − a$''^1\Sigma_g^+$ (2nd well) are shown in Figure 8. The calculated Einstein coefficients of the b$^1\Pi_u$ − a$''^1\Sigma_g^+$ (1st well) system are relatively strong and given in Table 4. The transition of the b$^1\Pi_u$ state to the a$''^1\Sigma_g^+$ (2nd well) is weak.

**Table 6.** Einstein coefficients ($s^{-1}$) for the $2^3\Delta_g - W^3\Delta_u$ and $2^3\Delta_g - H^3\Phi_u$ band transition systems of $N_2$.

| Transition system | $\upsilon'$ | 0 | 1 | 2 | 3 | 4 | 5 | 6 | 7 | 8 | 9 | 10 | 11 |
|---|---|---|---|---|---|---|---|---|---|---|---|---|---|
| | | | | | | | $\upsilon''$ | | | | | | |
| $2^3\Delta_g - W^3\Delta_u$ | 0 | $2.977 \times 10^{-1}$ | $8.351 \times 10^{0}$ | $1.102 \times 10^{2}$ | $9.164 \times 10^{2}$ | $5.419 \times 10^{3}$ | $2.438 \times 10^{4}$ | $8.704 \times 10^{4}$ | $2.532 \times 10^{5}$ | $6.116 \times 10^{5}$ | $1.242 \times 10^{6}$ | $2.138 \times 10^{6}$ | $3.137 \times 10^{6}$ |
| | 1 | $4.323 \times 10^{0}$ | $1.112 \times 10^{2}$ | $1.329 \times 10^{3}$ | $9.867 \times 10^{3}$ | $5.128 \times 10^{4}$ | $1.991 \times 10^{5}$ | $6.000 \times 10^{5}$ | $1.435 \times 10^{6}$ | $2.754 \times 10^{6}$ | $4.240 \times 10^{6}$ | $5.174 \times 10^{6}$ | $4.850 \times 10^{6}$ |
| $2^3\Delta_g - H^3\Phi_u$ | 0 | $6.081 \times 10^{1}$ | $2.160 \times 10^{2}$ | $2.996 \times 10^{2}$ | $2.032 \times 10^{2}$ | $6.794 \times 10^{1}$ | $9.081 \times 10^{0}$ | $2.340 \times 10^{1}$ | | | | | |
| | 1 | $3.782 \times 10^{2}$ | $8.600 \times 10^{2}$ | $5.701 \times 10^{2}$ | $6.901 \times 10^{1}$ | $2.285 \times 10^{1}$ | $6.860 \times 10^{1}$ | $2.356 \times 10^{1}$ | | | | | |

**Table 6.** Einstein coefficients ($s^{-1}$) for the $2^3\Delta_g - W^3\Delta_u$ band transition systems of $N_2$ (continued).

| Transition system | $\upsilon'$ | 12 | 13 | 14 | 15 | 16 | 17 | 18 | 19 | 20 | 21 | 22 | 23 |
|---|---|---|---|---|---|---|---|---|---|---|---|---|---|
| | | | | | | | $\upsilon''$ | | | | | | |
| $2^3\Delta_g - W^3\Delta_u$ | 0 | $3.940 \times 10^{6}$ | $4.244 \times 10^{6}$ | $3.921 \times 10^{6}$ | $3.100 \times 10^{6}$ | $1.874 \times 10^{6}$ | $1.058 \times 10^{6}$ | $5.032 \times 10^{5}$ | $1.997 \times 10^{5}$ | $6.473 \times 10^{4}$ | $1.651 \times 10^{4}$ | $3.094 \times 10^{3}$ | $3.640 \times 10^{2}$ |
| | 1 | $3.251 \times 10^{6}$ | $1.271 \times 10^{5}$ | $9.588 \times 10^{4}$ | $2.255 \times 10^{5}$ | $1.025 \times 10^{6}$ | $1.676 \times 10^{6}$ | $1.695 \times 10^{6}$ | $1.226 \times 10^{6}$ | $6.658 \times 10^{5}$ | $2.728 \times 10^{5}$ | $8.149 \times 10^{4}$ | $1.647 \times 10^{4}$ |

**Table 7.** Einstein coefficients (s$^{-1}$) for the $2^3\Sigma_u^+ - B^3\Pi_g$ band transition systems of N$_2$.

| $v'$ | $v''$ | | | | | | | | | | | | |
|---|---|---|---|---|---|---|---|---|---|---|---|---|
| | 0 | 1 | 2 | 3 | 4 | 5 | 6 | 7 | 8 | 9 | 10 | 11 | 12 |
| 0 | $3.053 \times 10^6$ | $4.654 \times 10^5$ | $4.036 \times 10^6$ | $2.642 \times 10^6$ | $1.462 \times 10^6$ | $7.271 \times 10^5$ | $3.368 \times 10^5$ | $1.480 \times 10^5$ | $6.219 \times 10^4$ | $2.502 \times 10^4$ | $9.688 \times 10^3$ | $3.660 \times 10^2$ | $1.383 \times 10^3$ |
| 1 | $6.877 \times 10^6$ | $2.263 \times 10^6$ | $2.551 \times 10^2$ | $1.044 \times 10^6$ | $2.032 \times 10^6$ | $2.013 \times 10^6$ | $1.468 \times 10^6$ | $8.990 \times 10^5$ | $4.940 \times 10^5$ | $2.527 \times 10^5$ | $1.225 \times 10^5$ | $5.666 \times 10^4$ | $2.510 \times 10^4$ |
| 2 | $6.580 \times 10^6$ | $2.391 \times 10^5$ | $2.988 \times 10^6$ | $1.515 \times 10^6$ | $4.251 \times 10^4$ | $4.033 \times 10^5$ | $1.184 \times 10^6$ | $1.453 \times 10^6$ | $1.244 \times 10^6$ | $8.719 \times 10^5$ | $5.392 \times 10^5$ | $3.068 \times 10^5$ | $1.643 \times 10^5$ |
| 3 | $3.399 \times 10^6$ | $4.206 \times 10^6$ | $1.127 \times 10^6$ | $6.907 \times 10^5$ | $2.061 \times 10^6$ | $9.892 \times 10^5$ | $4.178 \times 10^4$ | $2.298 \times 10^5$ | $7.941 \times 10^5$ | $1.084 \times 10^6$ | $1.022 \times 10^6$ | $7.833 \times 10^5$ | $5.282 \times 10^5$ |
| 4 | $9.814 \times 10^5$ | $5.181 \times 10^6$ | $7.445 \times 10^5$ | $2.870 \times 10^6$ | $4.712 \times 10^5$ | $9.820 \times 10^5$ | $1.512 \times 1$ | $6.365 \times 10^5$ | $2.360 \times 10^4$ | $1.654 \times 10^5$ | $5.830 \times 10^5$ | $8.385 \times 10^5$ | $8.401 \times 10^5$ |
| 5 | $1.356 \times 10^5$ | $2.228 \times 10^6$ | $3.915 \times 10^6$ | $1.176 \times 10^5$ | $2.566 \times 10^6$ | $9.487 \times 10^5$ | $8.957 \times 10^4$ | $1.076 \times 10^6$ | $1.103 \times 10^6$ | $4.012 \times 10^5$ | $8.612 \times 10^3$ | $1.376 \times 10^5$ | $4.552 \times 10^5$ |
| 6 | $1.368 \times 10^3$ | $2.658 \times 10^5$ | $2.429 \times 10^6$ | $1.469 \times 10^6$ | $1.631 \times 10^6$ | $1.238 \times 10^6$ | $1.699 \times 10^6$ | $1.343 \times 10^5$ | $3.756 \times 10^5$ | $9.948 \times 10^5$ | $7.870 \times 10^5$ | $2.430 \times 10^5$ | $1.275 \times 10^3$ |
| 7 | $7.434 \times 10^3$ | $1.372 \times 10^5$ | $1.186 \times 10^5$ | $1.252 \times 10^6$ | $2.621 \times 10^4$ | $3.761 \times 10^6$ | $3.734 \times 10^5$ | $1.422 \times 10^6$ | $7.973 \times 10^5$ | $2.851 \times 10^4$ | $5.349 \times 10^5$ | $8.621 \times 10^5$ | $5.264 \times 10^5$ |
| 8 | $5.577 \times 10^3$ | $9.571 \times 10^4$ | $3.693 \times 10^5$ | $1.683 \times 10^5$ | $1.610 \times 10^3$ | $1.894 \times 10^6$ | $8.517 \times 10^6$ | $8.259 \times 10^5$ | $6.274 \times 10^4$ | $2.753 \times 10^6$ | $4.808 \times 10^4$ | $1.364 \times 10^4$ | $1.034 \times 10^6$ |

## IV. Conclusion

In conclusion, the potential energy curves and the spectroscopic parameters of 7 singlet and 17 triplet electronic states of N$_2$ have been calculated using the icM-RCI + Q/56 + CV + DK method, and the radiative transition probabilities between different electronic states have been investigated using both the potential energy curves and the TDMs obtained by the icMRCI/AV6Z approach. The reproduced spectroscopic parameters are in excellent agreement with the experimental data, which manifests the accuracy of our calculated potential energy curves. Moreover, comparisons of the calculated vibrational levels and the inertial rotation constants with reliable experimental data for N$_2$ X$^1\Sigma_g^+$, A$^3\Sigma_u^+$, B$^3\Pi_g$, W$^3\Delta_u$, B$'^3\Sigma_u^-$, C$^3\Pi_u$, w$^1\Delta_u$, a$^1\Pi_g$ and a$'^1\Sigma_u^-$ states are also made, a good agreement within 1% is observed. To verify the accuracy and reliability of the obtained Einstein coefficients, the radiative lifetimes of the B$^3\Pi_g$, C$^3\Pi_u$ and W$^3\Delta_u$ states are calculated and compared with the experimental data, also a good agreement is observed. It is concluded that the present values of the Einstein coefficients in B$^3\Pi_g$ − A$^3\Sigma_u^+$, C$^3\Pi_u$ − B$^3\Pi_g$ and W$^3\Delta_u$ − B$^3\Pi_g$ transitions is reliable for astrophysical models. Such demonstrated quality of these observed transitions gives us confidence in the reliability of our predicted radiative transitions that were not observed in previous experiments, i.e. the $1^3\Sigma_g^-$ − C$'^3\Pi_u$, $2^3\Sigma_g^-$ − C$'^3\Pi_u$, $2^3\Sigma_g^-$ − B$'^3\Sigma_u^-$, $2^3\Delta_g$ − W$^3\Delta_u$, $2^3\Delta_g$ − H$^3\Phi_u$, $2^3\Sigma_u^+$ − B$^3\Pi_g$ and b$^1\Pi_u$ − a$''^1\Sigma_g^+$ transitions are predicted to be more intense due to the large Einstein coefficients. This work will provide guidelines for observing these predicted radiative transitions in the future.

## Disclosure statement

No potential conflict of interest was reported by the authors.

## Funding

## References

[1] J.W. Chamberlin, *Physics of the Aurora and Air Glow* (Academic Press Inc., New York, 1961).
[2] A.L. Broadfoot, S.K. Atreya, J.L. Bertaux, J.E. Blamont, A.J. Dessler, T.M. Donahue, W.T. Forrester, D.T. Hall, F. Herbert, J.B. Holberg, D.M. Hunten, V.A. Krasnopolsky, S. Linick, J.I. Lunine, J.C. McConnell, H.W. Moos, B.R. Sandel, N.M. Schneider, D.E. Shemansky, G.R. Smith, D.F. Strobel and R.V. Yelle, Science. **246**, 1459–1466 (1989).
[3] U.F. Harald, Rev. Geophys. **45**, 1–32 (2007).
[4] W.L. Imhof, E.E. Gaines, D.R. King, G.H. Nakano and R.V. Smith, Org. Lett. **7**, 573–576 (1964).

[5] A. Bogaerts, E. Neyts, R. Gijbels and J.V.D. Mullen, Spectroc. Acta. Pt. B-Atom. Spectr. **57**, 609–658 (2002).

[6] J. Anketell and R.W. Nicholls, Rep. Prog. Phys. **33**, 269 (1970).

[7] C.O. Laux, C.H. Kruger and J. Quant, Spectrosc. Radiat. Transf. **48**, 9–24 (1992).

[8] d.S. Lino and M.M. Dudeck, J. Quant. Spectrosc. Radiat. Transf. **102**, 348–386 (2006).

[9] Y. Babou, P. Rivière, M.-Y. Perrin and A. Soufiani, J. Quant. Spectrosc. Radiat. Transf. **110**, 89–108 (2009).

[10] R. Brun, *High Temperature Phenomena in Shock Waves* (Springer Berlin, Heidelberg, France, 2012).

[11] A. Lofthus and P.H. Krupenie, J. Phys. Chem. Ref. Data. **6**, 113–307 (1977).

[12] K.P. Huber and G. Herzberg, *Molecular Spectra and Molecular Structure IV. Constants of Diatomic Molecules* (Van Nostrand Reinhold, New York, 1979).

[13] D. Neuschäfer, C. Ottinger and A. Sharma, Chem. Phys. **117**, 133–148 (1987).

[14] L.G. Piper, K.W. Holtzclaw, B.D. Green and W.A.M. Blumberg, J. Chem. Phys. **90**, 5337–5345 (1989).

[15] M.E. Fraser, W.T. Rawlins and S.M. Miller, J. Chem. Phys. **88**, 538–544 (1988).

[16] C. Ottinger and A.F. Vilesov, J. Chem. Phys. **100**, 4862–4869 (1994).

[17] D. Cerny, F. Roux, C. Effantin, J. D''Incan and J. Verges, J. Mol. Spectrosc. **81**, 216–226 (1980).

[18] F. Roux, C. Effantin, J. D'Incan and J. Verges, J. Mol. Spectrosc. **91**, 238–242 (1982).

[19] F. Roux and F. Michaud, J. Mol. Spectrosc. **116**, 43–47 (1986).

[20] F. Roux and F. Michaud, J. Mol. Spectrosc. **129**, 119–125 (1988).

[21] F. Roux, F. Michaud and M. Vervloet, Can. J. Phys. **67**, 143–147 (1989).

[22] F. Roux and F. Michaud, Can. J. Phys. **68**, 1257–1261 (1990).

[23] F. Roux and F. Michaud, J. Mol. Spectrosc. **149**, 43–47 (1991).

[24] F. Roux, F. Michaud and M. Vervloet, J. Mol. Spectrosc. **97**, 43–47 (1993).

[25] B.R. Lewis, K.G. Baldwin, J.P. Sprengers, W. Ubachs, G. Stark and K. Yoshino, J. Chem. Phys. **129**, 164305 (2008).

[26] H.H. Michels, Adv. Chem. Phys. **45**, 225 (1981).

[27] W.C. Ermler, A.D. Mclean and R.S. Mulliken, J. Chem. Phys. **86**, 1305–1314 (1982).

[28] H.-J. Werner, J. Kalcher and E.-A. Reinsch, J. Chem. Phys. **81**, 2420–2431 (1984).

[29] W.C. Ermler, J.P. Clark and R.S. Mulliken, J. Chem. Phys. **86**, 370–375 (1987).

[30] H.J. Werner and P.J. Knowles, J. Chem. Phys. **89**, 5803–5814 (1988).

[31] P.J. Knowles and H.J. Werner, Chem. Phys. Lett. **145**, 514–522 (1988).

[32] H. Ndome, M. Hochlaf, B.R. Lewis, A.N. Heays, S.T. Gibson and H. Lefebvre-Brion, J. Chem. Phys. **129**, 164307 (2008).

[33] M. Hochlaf, H. Ndome, D. Hammoutène, M. Vervloet and J. Phys, B-At. Mol. Opt. **43**, 245101 (2010).

[34] M. Hochlaf, H. Ndome and D. Hammoutène, J. Chem. Phys. **132**, 104310 (2010).

[35] D.H. Shi, X. Wei, J.F. Sun, Z.L. Zhu and Y.F. Liu, Int. J. Quantum. Chem. **112**, 1323–1342 (2012).

[36] D.A. Little and J. Tennyson, J. Phys. B-At. Mol. Opt. **46**, 18592–18601 (2013).

[37] H.-J. Werner, P. J. Knowles, G. Knizia, F. R. Manby, M. Schütz, and others, MOLPRO, version 2015.1, a package of ab initio programs, < http://www.molpro.net > .

[38] H.-J. Werner, P.J. Knowles, G. Knizia, F.R. Manby and M. Schütz, WIRES Comput. Mol. Sci. **2**, 242–253 (2012) doi:10.1002/wcms.82.

[39] P.J. Knowles and H.J. Werner, Chem. Phys. Lett. **115**, 259–267 (1985).

[40] S.R. Langhoff and E.R. Davidson, Int. J. Quantum. Chem. **8**, 61–72 (1974).

[41] D.E. Woon and T.H. Dunning, J. Chem. Phys. **98**, 1358–1371 (1994).

[42] T.V. Mourik, A. Wilson and T. Dunningjr, Mol. Phys. **96**, 529–547 (1999).

[43] D.E. Woon and T.H. Dunning Jr, J. Chem. Phys. **103**, 4572–4585 (1995).

[44] G. Herzberg, *Molecular Spectra and Molecular Structure III* (Electronic Spectra and Electronic Structure of Polyatomic Molecules Van Nostrand Reinhold, New York, 1967).

[45] D. Spelsberg and W. Meyer, J. Chem. Phys. **115**, 6438–6449 (2001).

[46] D.G. Truhlar, Chem. Phys. Lett. **294**, 45–48 (1998).

[47] P.L. Fast, M.A.L. Sánchez and D.G. Truhlar, J. Chem. Phys. **111**, 2921–2926 (1999).

[48] M. Douglas and N.M. Kroll, Ann. Phys. **82**, 89–155 (1974).

[49] M. Reiher and A. Wolf, J. Chem. Phys. **121**, 10945–10956 (2004).

[50] M. Reiher and A. Wolf, J. Chem. Phys. **124**, 64102 (2004).

[51] R.J. Le Roy and J. Quant, Spectrosc. Radiat. Transf. **186**, 167–178 (2016).

[52] C.E. Moore, Nat Stand Ref Data Ser, Nat Bur Stand (US). **34**, 1–22 (1970).

[53] P.K. Carroll and R.S. Mulliken, J. Chem. Phys. **43**, 2170–2179 (1965).

[54] J.W. Ledbetter and K. Dressler, J. Mol. Spectrosc. **63**, 370–390 (1976).

[55] W. John and J. Ledbetter, J. Chem. Phys. **67**, 3400–3401 (1977).

[56] S.L. Guberman, J. Chem. Phys. **137**, 074309 (2012).

[57] H. Larsen, J. Olsen, P. Jørgensen and O. Christiansen, J. Chem. Phys. **113**, 6677–6686 (2000).

[58] T. Müller, M. Dallos, H. Lischka, Z. Dubrovay and P.G. Szalay, Theor. Chem. Acc. **105**, 227–243 (2001).

[59] W. Jiang and A.K. Wilson, J. Chem. Phys. **134**, 114104–65 (2011).

[60] R.E. Miller, J. Chem. Phys. **43**, 1695–1701 (1965).

[61] W.M. Benesch and K.A. Saum, J. Phys. B-At. Mol. Opt. **4** (1971).

[62] J. Kaplan, Phys. Rev. **45**, 947 (1934).

[63] A. Lofthus and R.S. Mulliken, J. Chem. Phys. **26**, 1010–1017 (1957).

[64] R. Mcfarlane, Ieee. J. Quantum. Elect. **2**, 229–232 (1966).

[65] U. Buontempo, S. Cunsolo, G. Jacucci and J.J. Weis, J. Chem. Phys. **63**, 2570–2576 (1975).

[66] A. Chutjian, D.C. Cartwright and S. Trajmar, Phys. Rev. Lett. **30**, 195–198 (1973).

[67] B.R. Lewis, A.N. Heays, S.T. Gibson, H. Lefebvre-Brion and R. Lefebvre, J. Chem. Phys. **129**, 164306 (2008).

[68] R.S. Freund, J. Chem. Phys. **50**, 3734–3740 (1969).

[69] P.K. Carroll, C.C. Collins and J.T. Murnaghan, J. Phys. B-At. Mol. Opt. **5**, 1634 (1972).

[70] D.E. Shemansky, J. Chem. Phys. **64**, 565–580 (1976).

[71] S. Chauveau, M.Y. Perrin, P. Rivière and A. Soufiani, J. Quant. Spectrosc. Radiat. Transf. **72**, 503–530 (2002).

[72] E.E. Eyler and F.M. Pipkin, J. Chem. Phys. **79**, 3654–3659 (1983).

[73] M. Larsson and T. Radozycki, Phys. Scripta. **25**, 627–630 (1982).

[74] M.N. Dumont and F. Remy, J. Chem. Phys. **76**, 1175–1176 (1982).

[75] K.H. Becker, H. Engels and T. Tatarczyk, Chem. Phys. Lett. **51**, 111–115 (1977).

[76] K.A. Saum, R. Covey and W. Benesch, J. Opt. Soc. Am. **63**, 592–596 (1973).

[77] R. Herman, Ann. Phys. **11**, 241–291 (1945).

[78] P.K. Carroll and N.D. Sayers, Proc. Phys. Soc. **66**, 1138 (1953).

[79] P.K. Carroll and A.P. Doheny, J. Mol. Spectrosc. **50**, 257–265 (1974).

[80] P.K. Carroll and C.P. Collins, Can. J. Phys. **47**, 563–589 (1969).

[81] G.K. James, J.M. Ajello, B. Franklin and D.E. Shemansky, J. Phys. B-At. Mol. Opt. **23**, 2055–2081 (1990).

[82] K. Dressler and B.L. Lutz, Phys. Rev. Lett. **19**, 1219–1221 (1967).

[83] B.L. Lutz, J. Chem. Phys. **51**, 706–716 (1969).